5-1-1989

Optically transparent IR reflective heat mirror films of ZNS-AG-ZNS

Bruce W. Smith

OPTICALLY TRANSPARENT IR REFLECTIVE HEAT MIRROR FILMS OF ZNS-AG-ZNS

by

Bruce W. Smith

A thesis submitted in partial fulfillment of the requirements for the degrees of Master of Science and Bachelor of Science in the Center for Imaging Science in the College of Graphic Arts and Photography of the Rochester Institute of Technology

May. 1989

Signature of the Author Bruce W. Smith

Center for Imaging Science

Accepted by _____ 8-9-89

Coordinator, M.S. Degree Program

ROCHESTER INSTITUTE OF TECHNOLOGY

CENTER FOR IMAGING SCIENCE

CERTIFICATE OF APPROVAL

The M.S. Degree Thesis of Bruce W. Smith
has been examined and approved
by the thesis committee as satisfactory
for the thesis requirement for the
Master of Science degree.

Dr. Vern Lindberg, Thesis Advisor

Bernt Hoppert

Dr. Roger Easton

THESIS RELEASE PERMISSION FORM

ROCHESTER INSTUTUTE OF TECHNOLOGY
COLLEGE OF GRAPHIC ARTS AND PHOTOGRAPHY

Title Of Thesis: Optically Transparent IR Reflective Heat Mirror Films of ZnS-Ag-ZnS.

I, Bruce W. Smith, hereby grant permission to the Wallace Memorial Library of R.I.T. to reproduce this thesis in whole or in part. Any reproduction will not be for commercial use or profit.

OPTICALLY TRANSPARENT IR REFLECTIVE HEAT MIRROR FILMS OF ZNS-AG-ZNS

by
Bruce W. Smith

Submitted to the
Center for Imaging Science
in partial fulfillment of the requirements
for the Master of Science and Bachelor
of Science degrees at the
Rochester Institute of Technology

ABSTRACT

Optically transparent heat mirror films, reflective in the infrared, have been produced based on a dielectric - metal - dielectric design using zinc sulfide and silver coatings. Filters exhibit 87% peak transmission in the visible region, while reflecting 80% in the infrared. Thermal testing indicated the that the layer filters were unstable to treatments above 300° F. Incorporation of thin barrier coatings of magnesium fluoride between the silver and zinc sulfide layers produced filters with thermal stability to 700° F while retaining optical characteristics of the three layer system. These optical and thermal properties offer possible application for the heat mirror films in tungsten source efficiency improvement applications.

Acknowledgements

Successful completion of this thesis was possible because of support from many sources. Valuable and timely assistance and advice was particularly appreciated from the following persons:

Dr. Vern Lindberg of the R.I.T. Physics Department, who acted as thesis advisor and provided a great deal of support and encouragement.

Bernt Hoppert, Jim Sternbergh, and their colleagues at Bausch and Lomb Optics Center for their guidance, technical assistance, and use of facilities and equipment.

Dr. Roger Easton of R.I.T. Center for Imaging Science.

Stephen Smith for help in upgrading vacuum coating equipment.

Dedication

To Dr. Ronald Francis

Table of Contents

List of Figures

List of Tables

Introduction

Radiation from incandescent sources in the long wavelength region results in a poor light-to-heat production ratio. Most incandescent emission falls beyond the limit of visual detection and into the infrared (IR), resulting in considerable heat production and poor luminous efficiency (radiant output weighted by visual sensitivity).

A tungsten filament, the most widely used source for incandescent lighting, radiates in wavelengths from 300 nm to 3500 nm (Figure 1) with peak radiation near 1000 nm and an average luminous efficiency of 7-10% [Stimson, 1974]. It's spectral distribution extends well beyond the visible range of 380-760 nm into the longer wavelength infrared region. By reducing the heat produced from the emission of long-wavelength radiation, the efficiency of a tungsten source could be substantially increased. Source performance would also improve in applications where heat build-up may be a problem. One way of achieving this heat reduction is by incorporating into the envelope of a tungsten lamp a thin film coating, transparent in the visible region but highly reflective in the infrared. Such a wavelength selective coating is known as a transparent heat mirror.

Transparent heat mirrors are thin films which allow transmission of visible light while reflecting IR radiation. A simple model of a heat mirror (Figure 2) demonstrates how

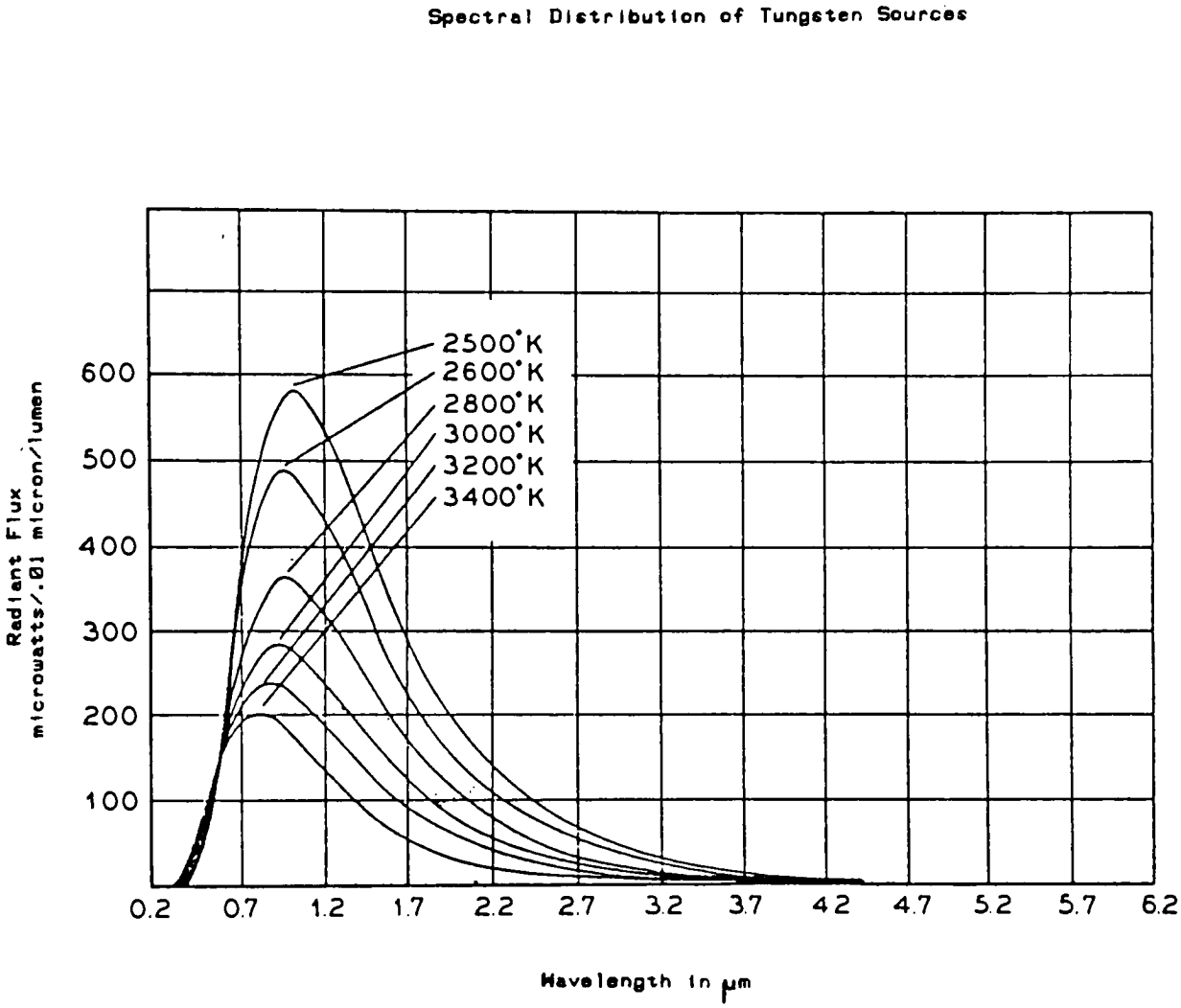
Spectral Distribution of Tungsten Sources
Radiant Flux
microwatts/.01 micron/lumen
600
500
400
300
200
100
2500°K
2600°K
2800°K
3000°K
3200°K
3400°K
0.2
0.7
1.2
1.7
2.2
2.7
3.2
3.7
4.2
4.7
5.2
5.7
6.2
Wavelength in μm

Figure 1

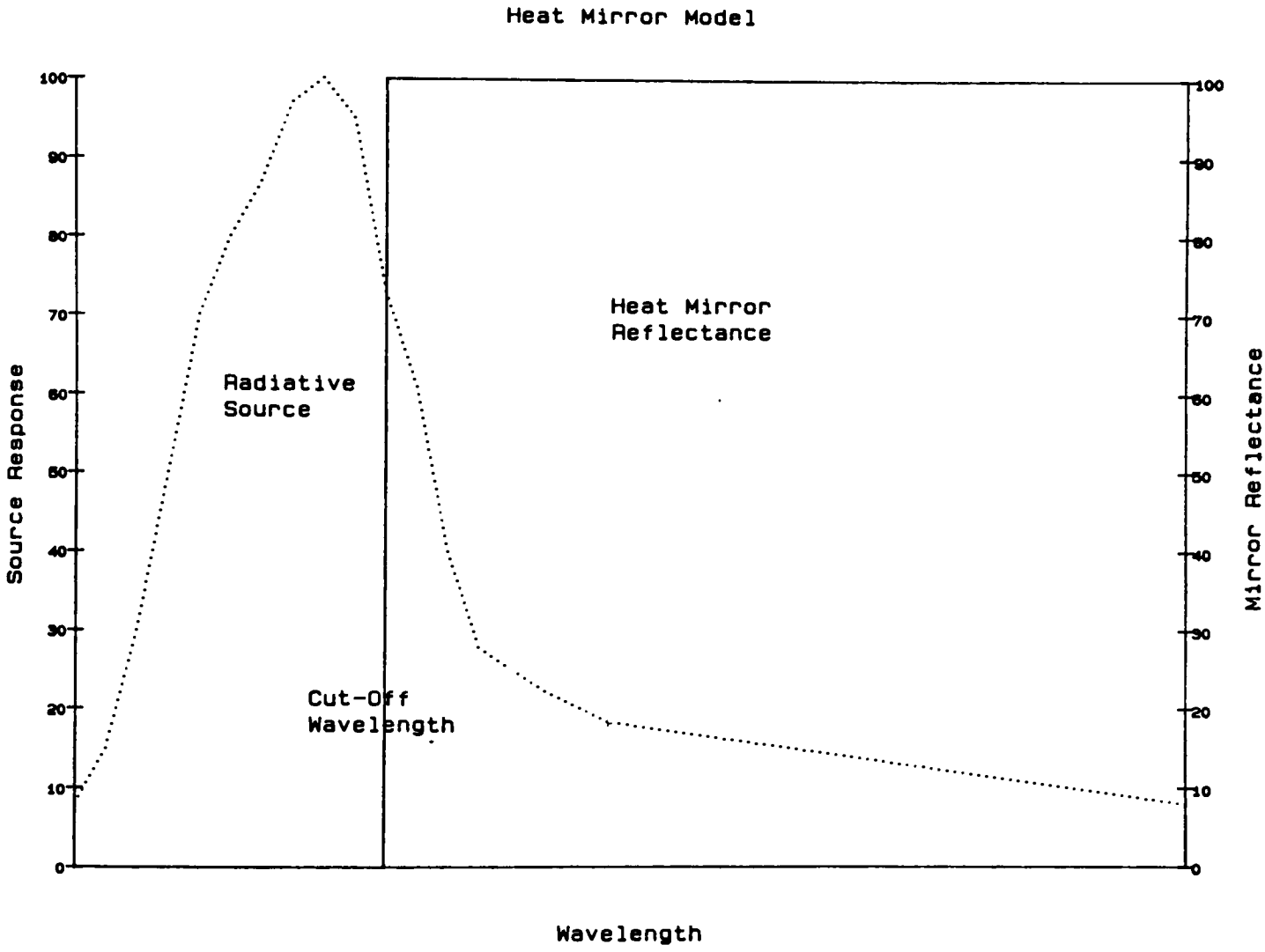
Heat Mirror Model
Source Response
Mirror Reflectance
Wavelength
Radiative Source
Heat Mirror Reflectance
Cut-Off Wavelength
100
90
80
70
60
50
40
30
20
10
0

Figure 2

operating wavelengths of a radiative source can be modified through selective transmission and reflection. By utilizing spectral characteristics of both the source and the heat mirror, system spectral emission can be predicted and optimized. Ideally, a heat mirror would have 100% transmission below and 100% reflection above a cutoff wavelength. All wavelengths below the cutoff would pass through the heat mirror while radiation of higher wavelengths would be reflected back to the source. The efficiency of a heat mirror for a specific application is determined by the relative position of the cutoff and the sharpness of the transition from transmission to reflection [Jarvinen, 1978].

Previously, all-dielectric interference filters have been used as heat mirrors [Macleod, 1969]. Short-wave pass filters have been designed which use stacks of dielectric layers of alternating high and low refractive indices. A variety of techniques have been developed to alter the range of reflectance wavelengths, including staggering layers to optimize optical thicknesses for several wavelengths. These all-dielectric filters not only require complex design techniques. There is also a need for great numbers of layers to produce desired characteristics. Designs with fifteen or more layers are common and up to sixty unique layers may be required for adequate heat reduction in some applications. [Thelen, 1963].

Other film types for transparent heat mirrors include semiconductors, thin-film microgrids, and metal films. Semiconductor films of interest exhibit three properties: (1) a sufficiently large energy band gap allowing transmittance in the visible region; (2) a limited number of excited levels within this gap; and (3) a free carrier concentration large enough to exhibit IR reflectance [Granqvist, 1981]. The spectral regions of transmission and absorption in a material are determined by interband transitions of intrinsic charge carriers across the energy band gap, E_g. The wavelength (in micrometers) at which transmission changes to absorption is equal to $1.23/E_g$ (eV). Band gaps larger than 2.5-3.0 eV are needed for visible transmission. Reflectivity of semiconductor materials in the infrared region can be increased by adding dopants, which generate free holes and electrons. These free carriers are excited by infrared radiation to interband transitions, resulting in reflectivity. The wavelength at which infrared reflectivity falls off (the plasma wavelength) is determined by the free carrier concentration, shifting to shorter wavelengths with increasing concentrations. Carefully prepared oxides of cadmium, tin, and indium exhibit proper band gaps for visible transmission, with adequate free carrier densities for infrared reflection achieved through controlled additions of dopants. Tin-doped indium oxide (ITO) films have been

studied for their optical and electrical properties [Hamberg, et al, 1981; Granqvist, et al, 1984; Agnihotri, et al. 1978].

Transparent heat mirrors for solar energy applications have been fabricated by chemically etching tin-doped indium oxide to form transparent conducting microgrids. These electromagnetic filters are essentially a thin film metal wire mesh. With openings of approximately 2.5 um on a side and linewidths of sub-micron size, visible radiation is transmitted while IR reflectivity remains high [Fan, Bachner, Murphy. 1976]. Fabrication of these films has been difficult, however.

Metal-film heat mirrors utilize a thin metal film reflective in the infrared but with low enough visible absorption to allow optical transmission [Hass. 1956]. By maximizing transmission in the visible region and retaining high reflection in the infrared, metal films can be utilized as efficient heat mirrors. This study investigates the potential utilization of the wavelength selective properties of thin metal films as heat mirrors.

Reflection in thin metal films depends on the optical properties of the material and on the wavelength of incident radiation. Metals with low refractive indices and high extinction coefficients have potential for the IR. A detailed approach to reflectivity in metal films is included in Appendix 1.

Absorotion in thin metal films is a function of conductivitv. The electrons in a metal with ideal infinite conductivitv are driven into oscillatıon bv an impinging harmonic wave. These electrons are comoletelv free to circulate within the material. There would be no restoring force within the material and, therefore, no absorption. In real metals however, where conductivitv is finite, absorotion occurs as conduction electrons underqo collisions and convert electromagnetic energv to heat.

Absorotion in a thin film can be calculated from Lambert's Law:

$$I(t)/I_o = e^{-at}, \quad (1)$$

where $I(t)$ is transmitted intensity, I_o is incident intensity, t is film thickness and a is the absorotion coefficient of the material. Absorotion in a film decreases exponentiallv with t. It can be seen that an IR reflective film just thick enough to be continuous would remain somewhat transparent and could be used as a heat mirror.

Cooper, gold, and silver are metals which reflect well in the IR region. As seen from the plot of absorotion vs. wavelength in Figure 3, copper and gold absorb approximatelv 50% of the incident radiation at wavelengths below 500 nm,

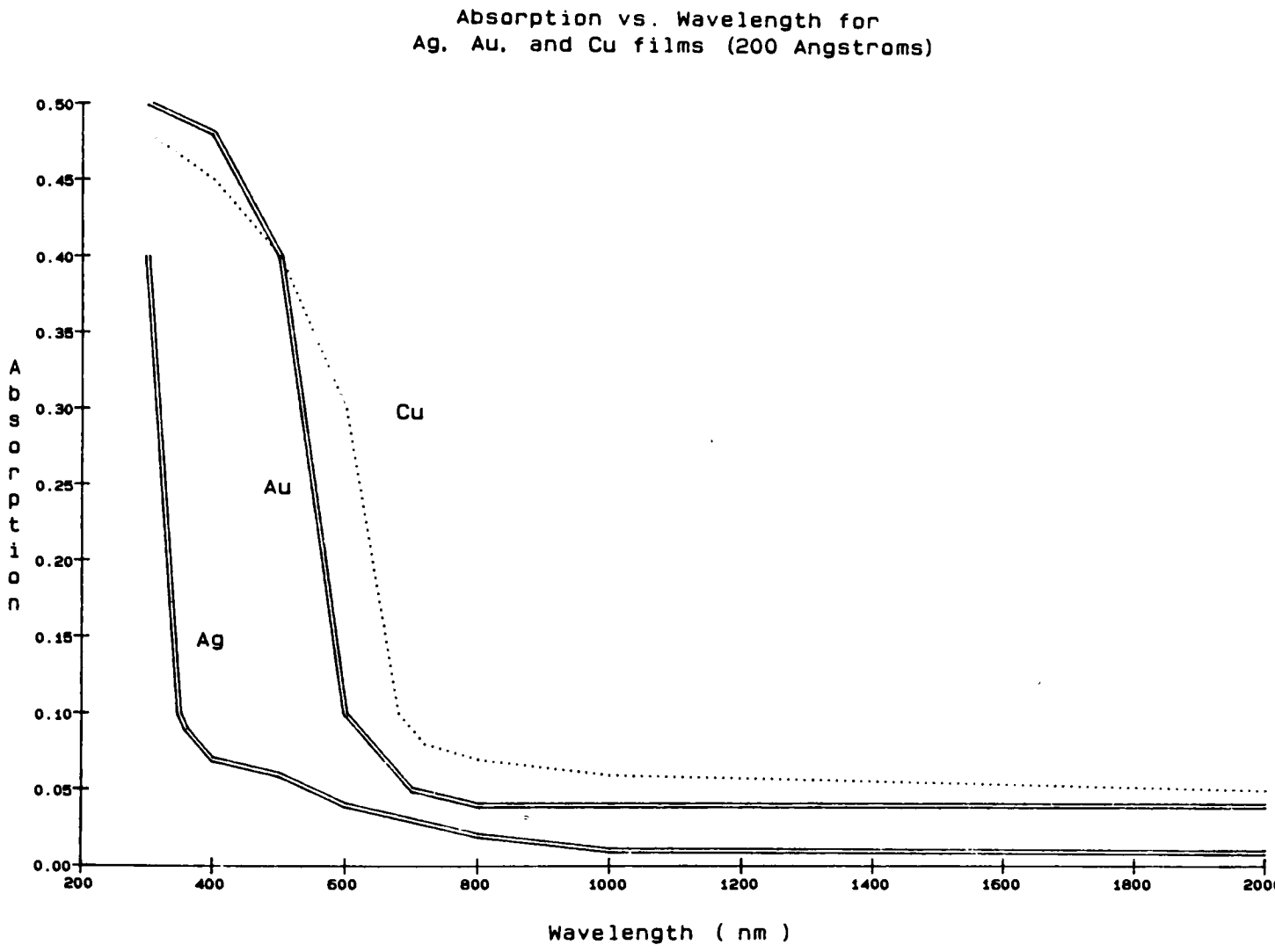
Absorption vs. Wavelength for
Ag. Au. and Cu films (200 Angstroms)
Absorption
0.50
0.45
0.40
0.35
0.30
0.25
0.20
0.15
0.10
0.05
0.00
Cu
Au
Ag
200
400
600
800
1000
1200
1400
1600
1800
2000
Wavelength (nm)

Figure 3

while silver shows little absorption above 300 nm. This relatively low visible absorption makes silver a much more suitable metal than copper or gold as a heat mirror [Fan, Bachner. 1976].

Transmission at short wavelengths can be further enhanced in metals by supressing reflection with appropriately designed interference coatings. Through the use of a single-layer dielectric film approximately one-quarter optical wavelength thick, visible transmission in metals has been shown to increase, [Hass. 1955]. Metal films sandwiched between two coatings of dielectric materials have been shown to possess even higher visible transparency [Holland and Siddall, 1958]. Fan, et al. [1974, 1976] found that thin films of silver deposited between two layers of titanium dioxide possess excellent heat mirror characteristics. Three-layer $TiO_2/Ag/TiO_2$ coatings exhibited both high visible transmission (84%) and high infrared reflection (98%). Filters were stable and showed no optical degradation when subjected to heating up to 600° F.

Other dielectric materials have been studied for use with thin metal films. Films of Bi_2O_3 [Holland and Siddel, 1958], SiO [Holland and Siddel, 1958], ZnO [Glaser, 1980], and ZnS [Groth and Kauer, 1965] have been investigated.

The main criterion for selecting a dielectric material for use with metal films is a high refractive index. As the

refractive index of the dielectric material increases, short-wavelength reflection is decreased and better heat mirror characteristics can be achieved [Hass, 1956]. Reflectivity of a metal of index $n-ik$ coated with a single dielectric layer of index $n(1)$ and thickness $t(1)$ can be calculated as [Smith, 1966]:

$$R = \frac{r(1)^2 + r(2)^2 + 2r(1)r(2)\cos(X)}{1 + r(1)^2 r(2)^2 + 2r(1)r(2)\cos(X)} \quad (2)$$

where:

$$X = \frac{4\pi n(1)t(1)\cos I(1)}{L},$$

$$r(1) = \frac{1 - n(1)}{1 + n(1)}, \text{ and}$$

$$r(2) = \frac{n(1) - (n(2) - ik)}{n(1) + (n(2) - ik)}.$$

at normal incidence, where $I(0) = I(1) = I(2) = 0$ in Figure 4.

Figure 5 shows effects of dielectric film index on a metal film. Reflectance is calculated for quarter-wave films (546 nm) of increasing refractive index [Hass, 1956]

Since the effectiveness of a heat mirror also depends on its stability, the dielectric material must also produce a stable filter system in combination with the metal for conditions to which the heat mirror will be subjected. Any filter combination must possess chemical stability to

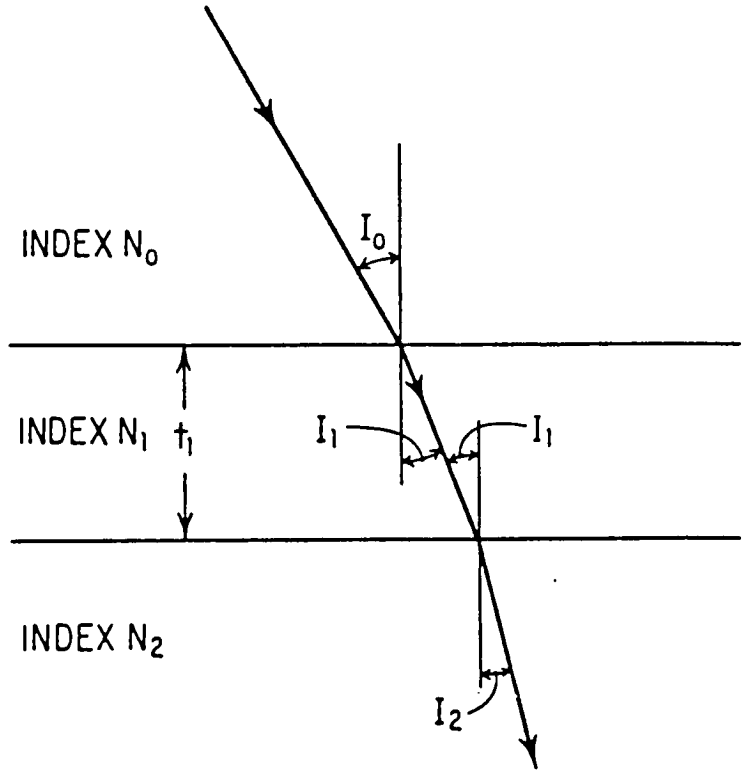

Passage of a light ray through a thin film [Smith, 1966].

Figure 4

Reflectance of Aluminum Film with
Single Dielectric Coating of Increasing Refractive Index
(546 nm wavelength)

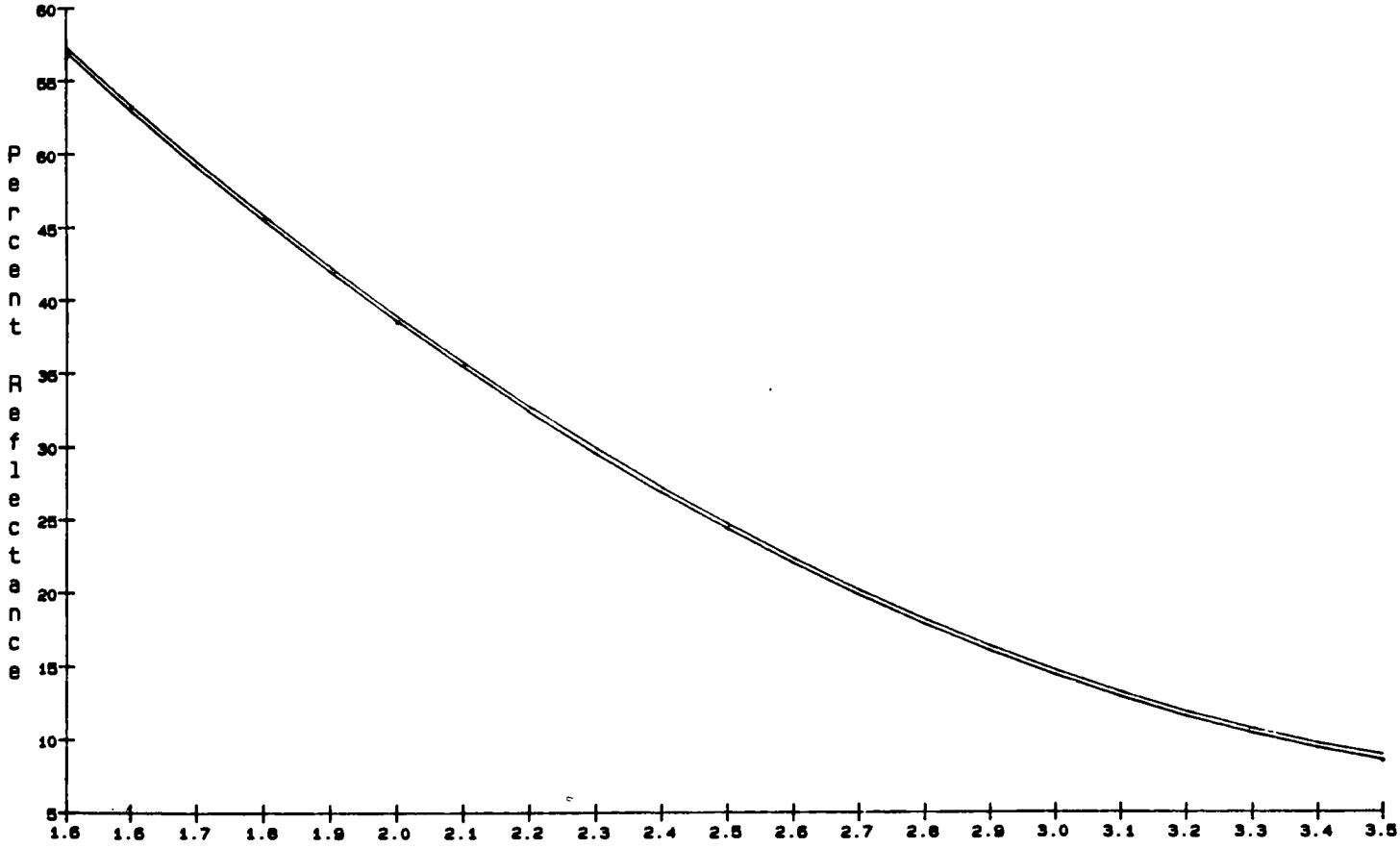

Figure 5

withstand environmental conditions, system operating temperatures, etc.

Both zinc sulfide and titanium dioxide have large refractive indices when compared to other materials transparent in the visible region. Values are near 2.5 for both materials [AIP, 1972]. Titanium dioxide in combination with silver has been shown to exhibit excellent heat-mirror spectral characteristics and chemical resistance [Yoldas and O'Keefe, 1984], but little work has been done in these areas with zinc sulfide. Although this material has the potential for good heat mirror spectral characteristics, its stability and suitability in a dielectric / metal / dielectric heat mirror need further study.

The objective of this research was to develop a stable transparent heat mirror suitable for use with incandescent light sources using dielectric / metal / dielectric layers. It is a system which involves no complex design techniques and has high heat reduction and stability potential. Silver has been shown to possess low absorption characteristics in the visible region and high reflection in the IR. Zinc sulfide has the optical characteristics needed for dielectric interference layers. The combination of these materials, and the optimization of a system incorporating them, has been the intent of this study. Additional concerns included the following.

1. Stability problems are inherent at a silver / sulfide interface. Silver combines readily with sulfur to form silver sulfide (heat of formation of -7.79 kcal/mol at 25°C. compared to ZnS = -49.23 kcal/mol [CRC Handbook. 1984]) and any heating of the filters may cause degradation at that interface. The cause and severity of any stability problems (after coating and at elevated temperatures), needed study.

2. Improvement upon any limitations of a silver / zinc sulfide filter required investigation. Thin barrier layers coated between the silver and zinc sulfide were considered to isolate interface interactions. Magnesium fluoride's ability to form hard, durable, and stable films makes it a good candidate for barrier use. With an index of refraction of 1.38. it is commonly used for protective anti-reflection coatings. Its ability to isolate possible ZnS and Ag interactions and its effects on optical performance in a dielectric / metal / dielectric heat mirror system needed investigation.

The development of a working heat mirror utilizing these designs and materials is expected to encourage further investigation into the practical applications of heat reduction in incandescent light sources.

Experimental

Spectral requirements were determined for an effective heat mirror for use with an incandescent light source. From the spectral characteristics of a tungsten source (Figure 6) and the range of the visible spectrum (Figure 7), a target spectral response, with appropriate transmission values, was determined for a heat mirror filter. Highest transmission was desired in the range where maximum human visual response occurs. Highest reflection was desired where tungsten emission falls beyond the visible region. The target response was then used for design goals in determining multilayer filter characteristics (Figure 8).

Both analytical and computer-aided techniques are available designing and analyzing thin film systems. Spectral characteristics of a system with known optical thicknesses can be calculated using a matrix-type approach which is handled easily with minimal computation [Macleod, 1969]. A computer program, written in BASIC, was utilized to handle such an analysis, determining transmission and reflection values (from non-absorbing materials), and is contained in Appendix II. In designing a thin film system based on a specified spectral response, the determination of optical thicknesses is a problem of much greater complexity and would involve lengthy computations if not handled by a computer. Using a Hewlett-Packard based computer system

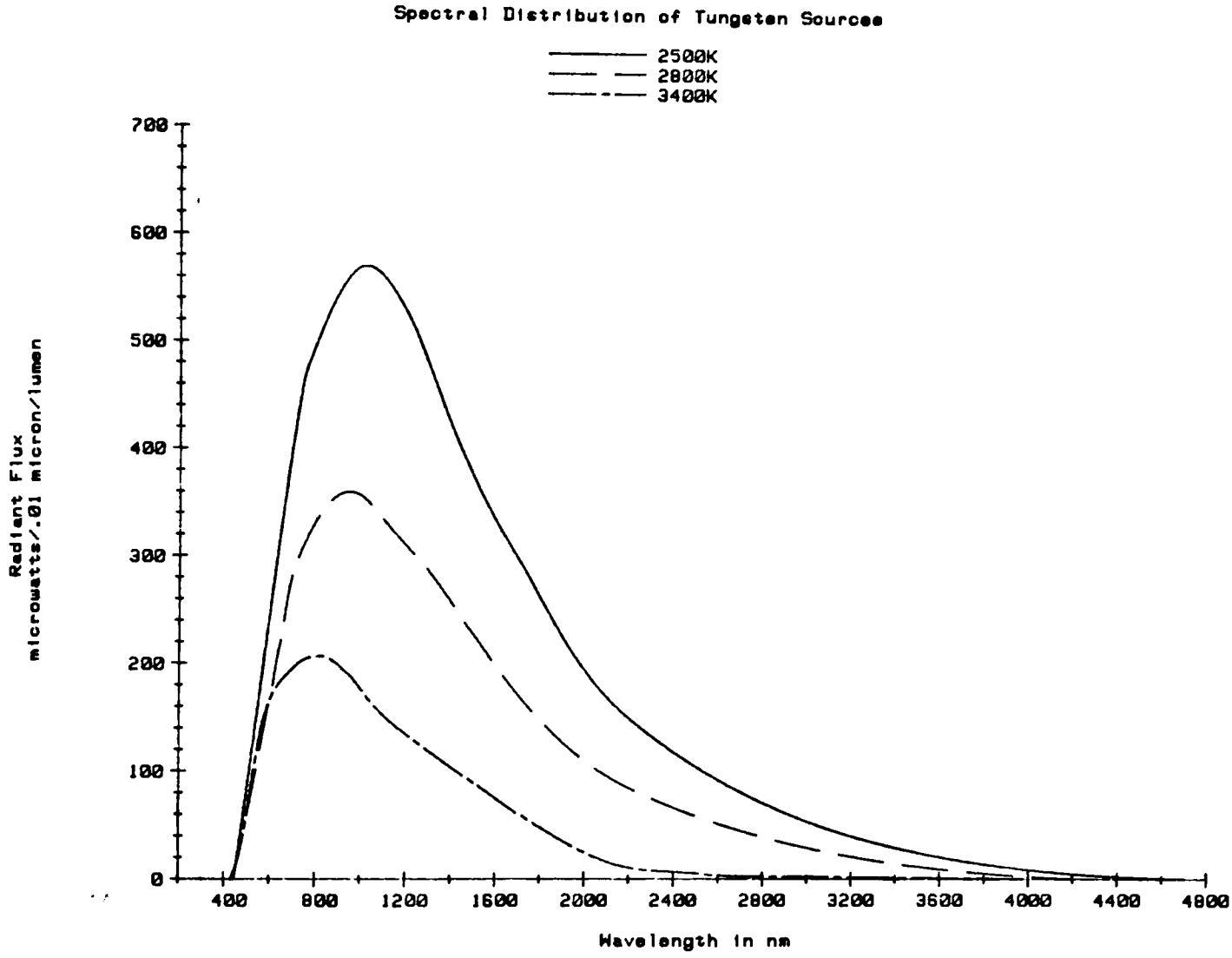
Spectral Distribution of Tungsten Sources
2500K
2800K
3400K
Radiant Flux
microwatts/.01 micron/lumen
700
600
500
400
300
200
100
0
400
800
1200
1600
2000
2400
2800
3200
3600
4000
4400
4800
Wavelength in nm

Figure 6

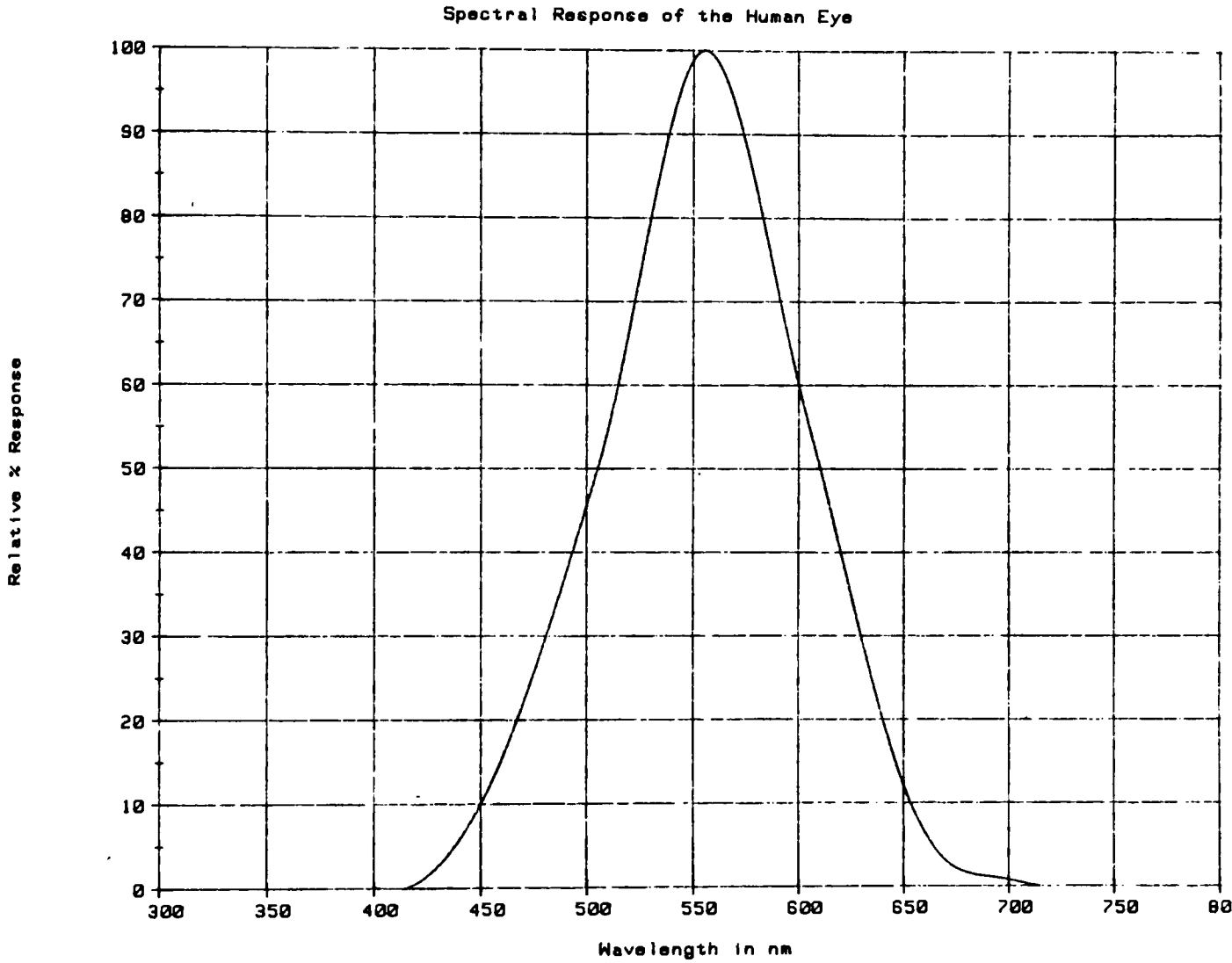
Spectral Response of the Human Eye
Relative % Response
100
90
80
70
60
50
40
30
20
10
0
300
350
400
450
500
550
600
650
700
750
800
Wavelength in nm

Figure 7

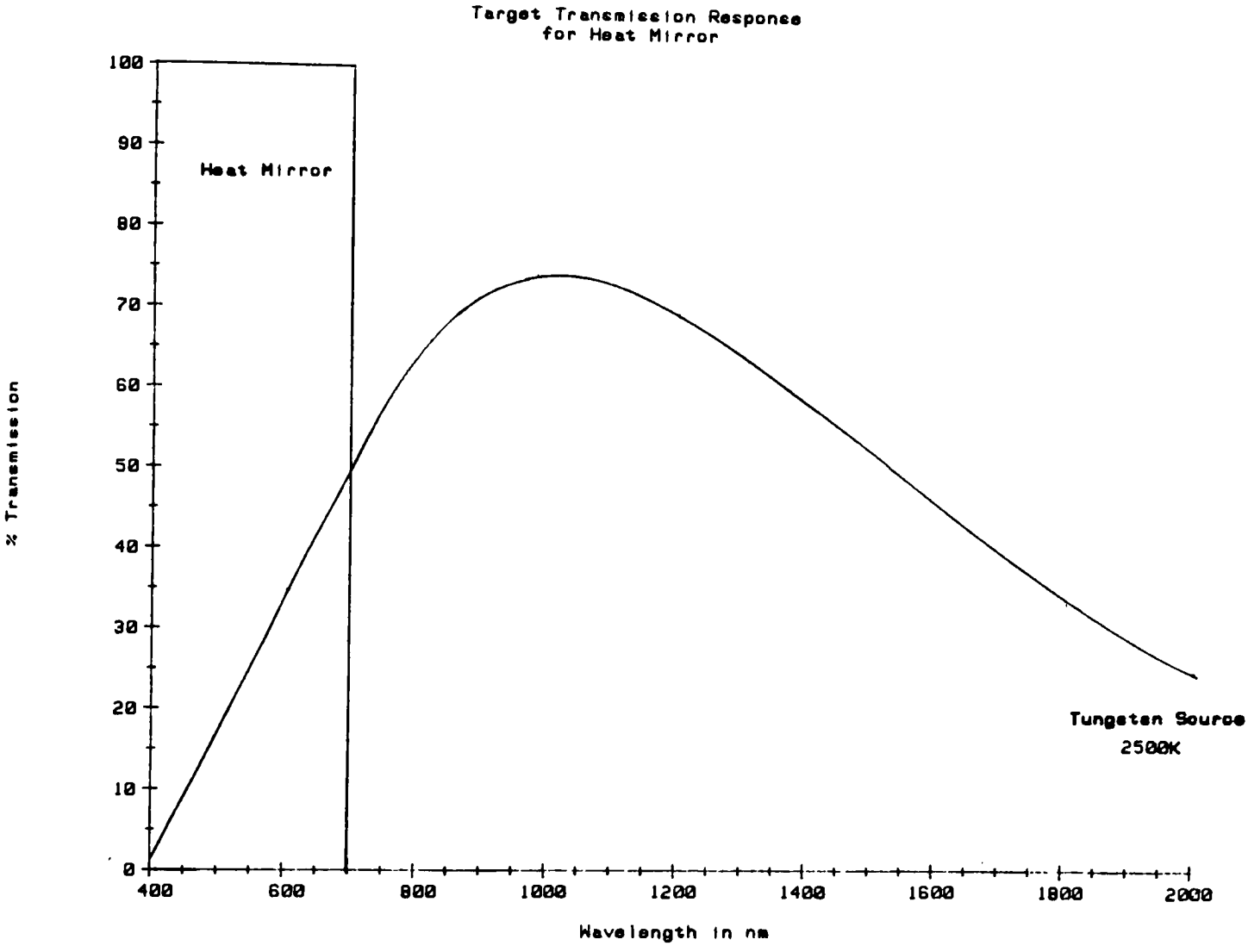
Target Transmission Response
for Heat Mirror
Heat Mirror
Tungsten Source
2500K
% Transmission
Wavelength in nm
100
90
80
70
60
50
40
30
20
10
0
400
600
800
1000
1200
1400
1600
1800
2000

Figure 8

with an optical thin films software package (Film-Star), computer optimization was possible with a starting design, material constants, and targeted spectral characteristics.

Bulk properties of materials (silver and zinc sulfide) were used for optical constants in computer optimizations. The optical constants of thin films differ greatly from bulk properties and deposition parameters affect actual values, but these starting values provided initial designs which could be optimized through experimentation. An initial starting design, before optimization, of 150Å of silver with 1/4 optical wavelength (a product of wavelength of interest and refractive index)of zinc sulfide (570Å thickness at 550 nm) on each side was chosen. Spectral analysis of this initial design showed high transmission in the visible region but low reflection values in the infrared region. Computer optimization was run on this design to yield a configuration to closely match the target conditions, with optimum thicknesses for the silver and zinc sulfide layers. Random thickness tolerance tests were run on this design to simulate error effects during coating. Thickness tolerance designs with 20 % and 40% maximum error were simulated.

Films were deposited in a CVC vacuum system modified for deposition of two materials in a single pump-down. The vacuum system is capable of maintaining a vacuum of 2×10^{-5} torr. The system is equipped with a quartz deposition monitor placed to maintain a 1:1 tooling ratio during

coating. Calibration of the deposition monitor was performed using gravimetric methods and periodic calibration checks were made. A rotating shutter was built into the system for accurate deposition and cutoff of thin films. All films were deposited on glass 1" x 3" slides by resistive thermal evaporation in vacuum. ZnS and Ag were deposited from Tantalum boats, MgF_2 was deposited from a tungsten boat.

Since the thinnest possible continuous silver film is required for maximum transmission, coating conditions affecting film growth had to be addressed and determined. Nucleation begins at point defects in the substrate and atoms cluster to form islands at these sites [Venables. Spiller, Hanbucken, 1984]. If large islands are formed (with large interisland spacing) light scattering dominates over transmission and thicker films must be deposited to obtain continuity. To reduce this agglomeration, early film coalescence is required. Several factors determine the island size and spacing. Elevated substrate temperatures will increase the mobility of arriving atoms, allowing for migration to sites of large island formation. High deposition rates have the same effect by increasing the arriving vapor flux density. This increases the probabilities of capture at existing sites or nucleation of atom clusters at new sites. Increased agglomeration is also achieved when the deposition angle is off normal axis to the

substrate. Greater lateral mobility is possible and large island growth is likely. To determine an optimum deposition rate, a series of filters were coated at rates of 2, 6, 10, and 20Å/second and compared. All coatings were condensed at room temperatures and at normal incidence. To determine continuity of metal films, conductivity tests, using a digital ohm-meter, were made at all metal thicknesses throughout experimentation. Once coating factors were determined, single-layer silver films were deposited starting at the computer optimized thickness. A Beckman Spectrophotometer UV 5240 (from Bausch and Lomb Vacuum Coating Division), capable of measurements from 200 nm to 2000 nm, was used to measure spectral response. Films were coated at decreasing thicknesses until a silver coating was achieved which was as thin as possible but remained uniform and continuous with high visible transmission.

Additionally, two-layer coatings were produced with ZnS/Ag (from substrate) based on the computer optimized design as well as silver thicknesses determined experimentally. ZnS layers were varied from the initial design thicknesses until optimum results were achieved in combination with the thin silver film. Visual inspection allowed for this optimization with high visible transmission as the criterion. Filters were then spectrophotometrically measured. From this work, three-layer coatings were made with ZnS, Ag, and ZnS. ZnS films thicknesses determined

from two layer formulations were appropriately coated on either side of a thin silver film. Measurements were made on these three layer coatings and compared with results from single and two-layer filters. Layer thicknesses were varied for each of the three layers until adequate heat mirror characteristics were obtained.

To determine stability of the three-layer filters a series of heat tests were performed. This heat testing was performed to determine the stability of the filters with age, and determine the extent to which the filters could withstand high temperature conditions. The temperature limits on these filters provided criteria for stability comparisons with other filter designs (particularly the $TiO_2/Ag/TiO_2$ filter of Fan, et al [1974, 1976]). Filters were heat treated for one hour at temperatures starting at 300° F and increasing by 200° F increments until degradation. Filter degradation was determined by IR transmission characteristics. Filters were no longer useful as heat mirrors when IR transmission rose above average visible transmission.

The optical effects of thin barrier layers of magnesium fluoride between the ZnS and Ag layers was tested using Film-Star thin films software on the Hewlett-Packard computer. The five layer design became $ZnS/MgF_2/Ag/MgF_2/ZnS$, on glass in air. Interlayer thicknesses were determined so that the new five-layer design would retain adequate

transmission characteristics while providing isolation between the silver and zinc sulfide layers. Initial depositions of the five layer design had barrier layers coated thinner than the computer optimized values in order to determine minimal MgF_2 thicknesses. Magnesium Fluoride thicknesses of 5, 10, and 20Å were coated at approximately 2-5Å/S and spectral response was determined. Heat tests were conducted on these samples as with three-layer filters and stability limits were determined.

Inadequacy of these MgF_2 thicknesses to increase stability of the filter prompted further testing on individual layers to determine the mechanism of failure. Combinations of 80Å of MgF_2 on 100Å, 150Å, and 250Å of Ag were coated to determine if MgF_2 was interacting with Ag to deplete the metal layer thickness into discontinuity. Negative results in this area lead investigation into continuity problems of the MgF_2 layer itself. Barrier film thickness and deposition rate were both areas of suspect. Thicker layers of MgF_2 (approximately three times previous thicknesses) were coated in the five layer design at deposition rates of 12-20Å/S. These filters were optically measured and compared to three layer design for suitable heat mirror characteristics.

These films were subjected to heat testing starting at 400° and continuing at 100° F intervals until failure. Filters were measured spectrophotmetrically and any changes

caused by heating were recorded. Any substantial effects of the barrier layers on stability and spectral characteristics were determined.

Results

Computer analysis of the initial ZnS/Ag/ZnS design of 1/4 optical wavelength ZnS on 150Å Ag yielded a calculated average visible transmission of 64% with a maximum of 91% near 700 nm. High transmission also extended well into the IR region and a well defined cut-off edge did not exist (Figure 9). Computer optimization of this initial design showed increased visible transmission, increased IR reflection, and better edge characteristics (Figure 10). Final design thicknesses were 227Å Ag between two 336Å layers of ZnS (.147 optical wavelength with 550 nm radiation), using bulk material properties for optical constants [AIP. 1972]. Random tolerance tests on this design (Figures 11 and 12) simulate coating thickness error and show adequate allowances for thickness variations. Random tolerance analysis simulates coating error and variations, showing both 20% and 40% maximum error to produce suitable heat mirror films.

Silver deposition rates were partially limited by the capability of the system. Difficulty was encountered at high rates (greater than 20Å/S) when coating thin films due to time constraints on shutter operation. Accurate thicknesses became difficult because of errors imposed by manual shutter operation at these high deposition rates. Table 1 contains calculated thickness errors at various

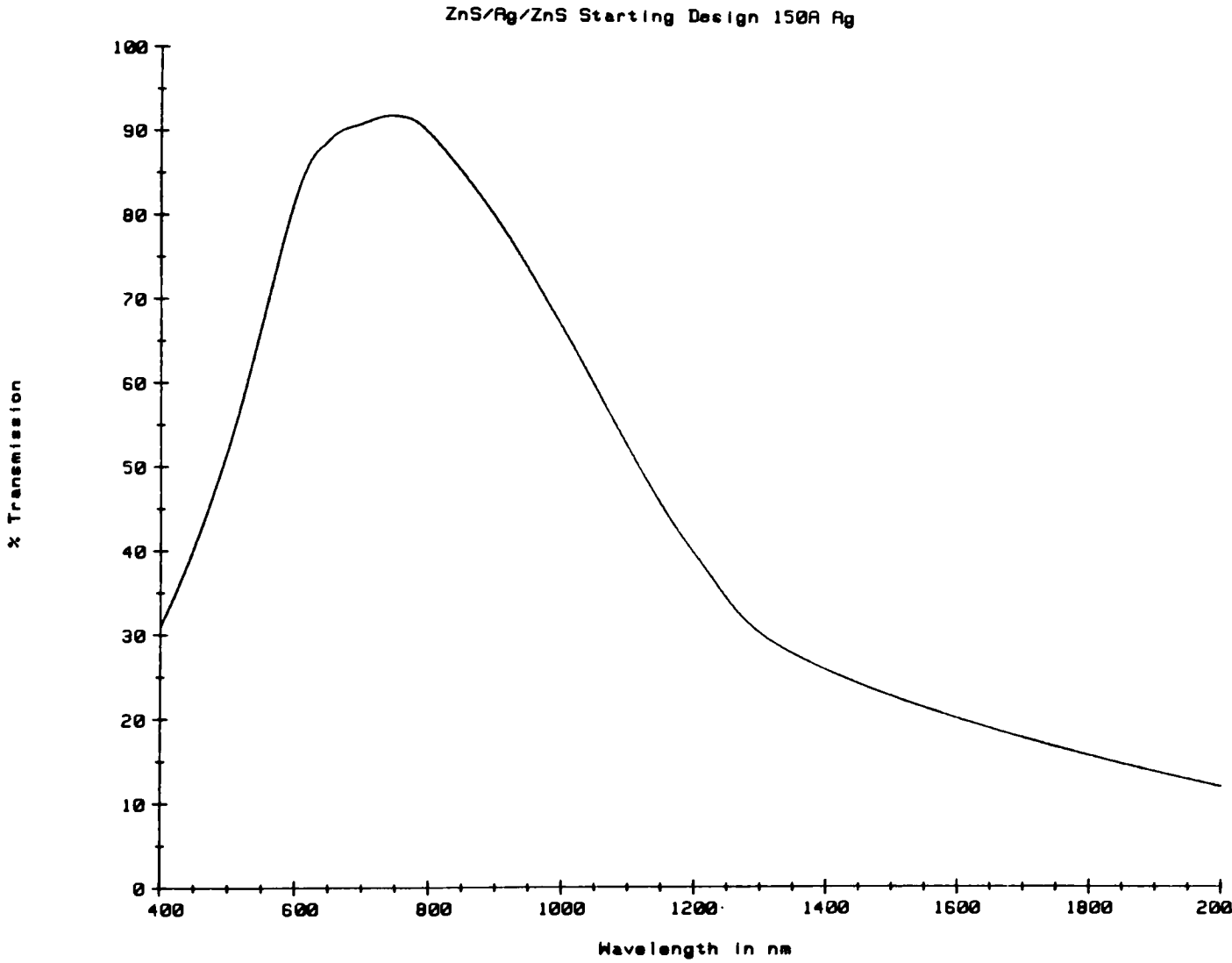
ZnS/Ag/ZnS Starting Design 150Å Ag
% Transmission
100
90
80
70
60
50
40
30
20
10
0
400
600
800
1000
1200
1400
1600
1800
2000
Wavelength in nm

Figure 9

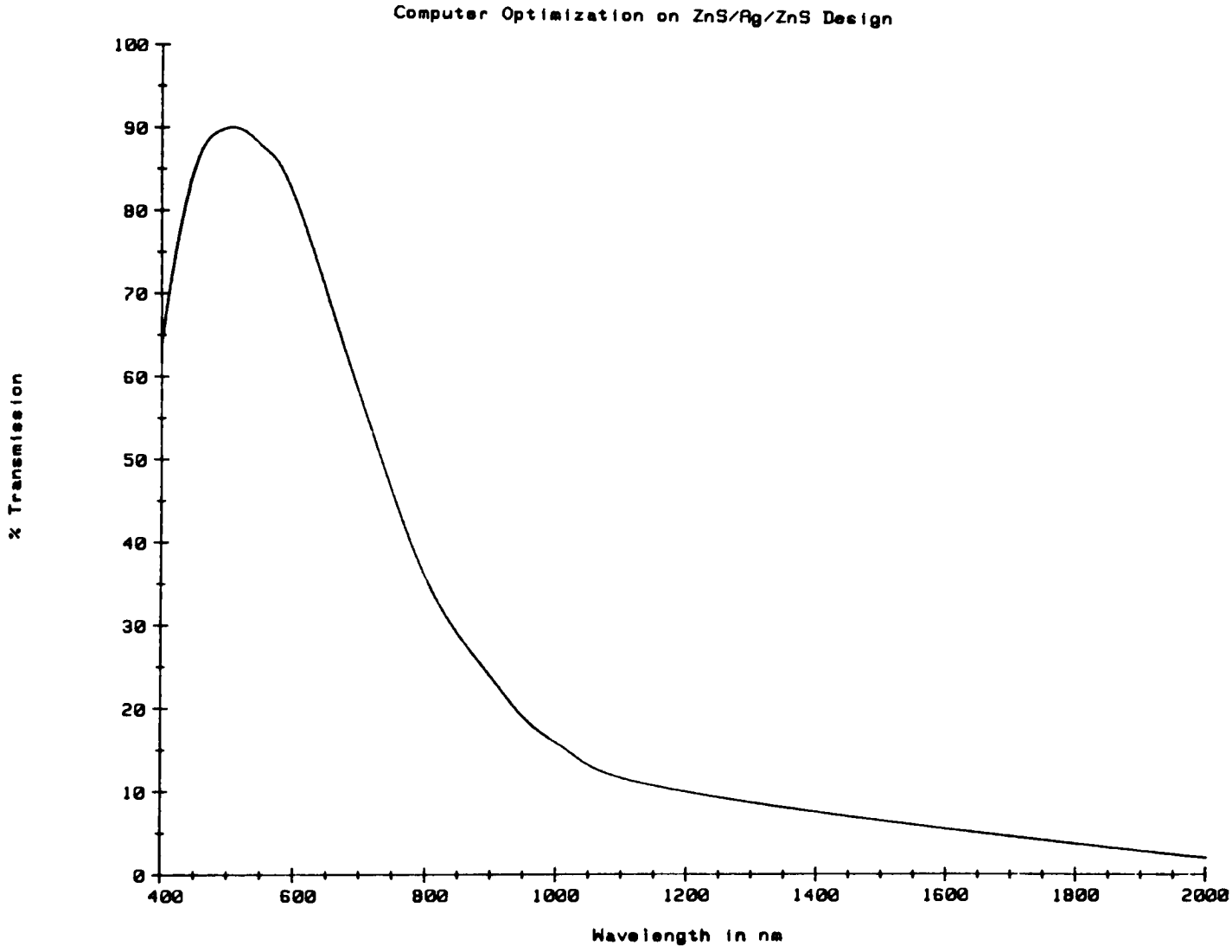
Computer Optimization on ZnS/Ag/ZnS Design
% Transmission
100
90
80
70
60
50
40
30
20
10
0
400
600
800
1000
1200
1400
1600
1800
2000
Wavelength in nm

Figure 10

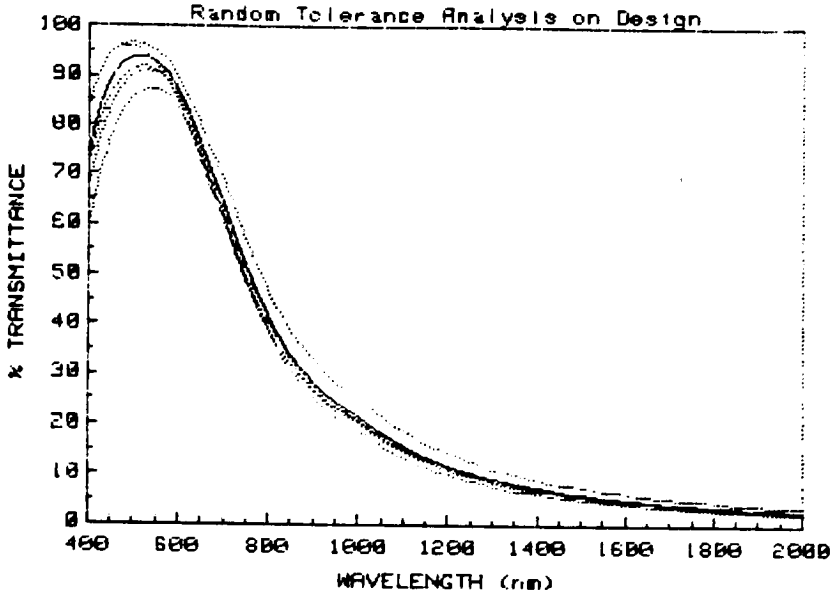

20% Random Tolerance Tests on Design

Figure 11

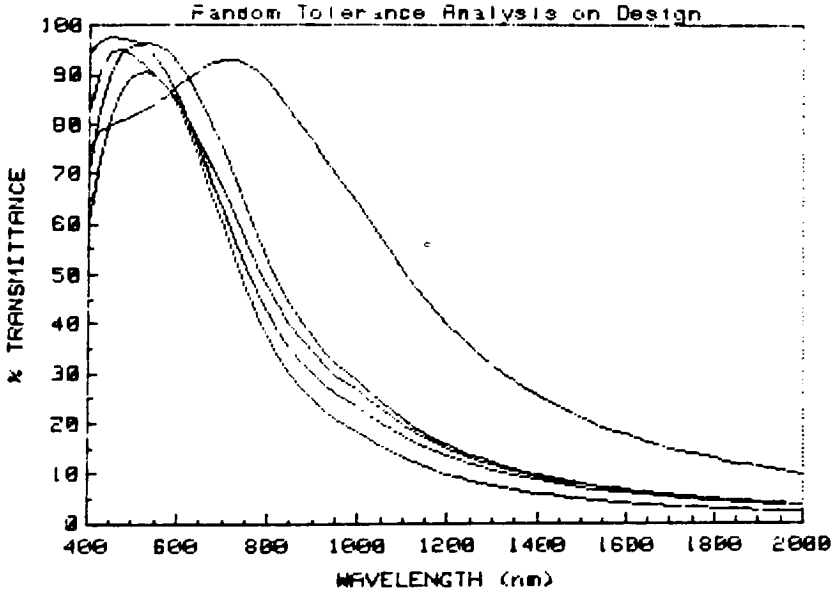

40% Random Tolerance Tests on Design

Figure 12

TABLE 1

Calculated Thickness Errors at Various Coating Rates

Deposition Rate	Time to Move Shutter	Thickness Error
10 A/sec	0.5 sec	5 A
15	"	8
20	"	10
25	"	13

coating rates. Rates of 2, 6, and 10Å/S produced similar optical properties in silver films, any differences were attributed to thickness variations. Since very low rates may have lead to a greater influence from impurities and gas inclusions, 15-20Å/S was chosen as a practical rate for Ag deposition.

Coating single layer silver films of 220Å Ag resulted in filters with dark gray coloration and poor visible transmission.

Optimum characteristics were obtained with 85Å thicknesses. These continuous films appeared light gray and moderately transparent. Figure 13a shows transmission characteristics from 300 nm to 2000 nm. Silver films of 70Å and 65Å were also produced but coating uniformity was inferior to 85Å thick filter.

ZnS thickness for two layer Ag/ZnS coatings showed optimum transmission characteristics at 320Å +/-30Å when over-coated by 85Å Ag . Thicknesses greater than this (up to 800Å) resulted in dark blue coatings with poor visible transmission (visually inspected). Figure 13b shows the transmission characteristics for the two-layer Ag(85Å) over ZnS(300Å) on glass.

Three-layer filters of 330Å ZnS, 85Å Ag, and 320Å ZnS were produced based on one and two-layer thicknesses and the computer optimized design. Figure 13c shows the spectral characteristics of this filter, compared to those of the

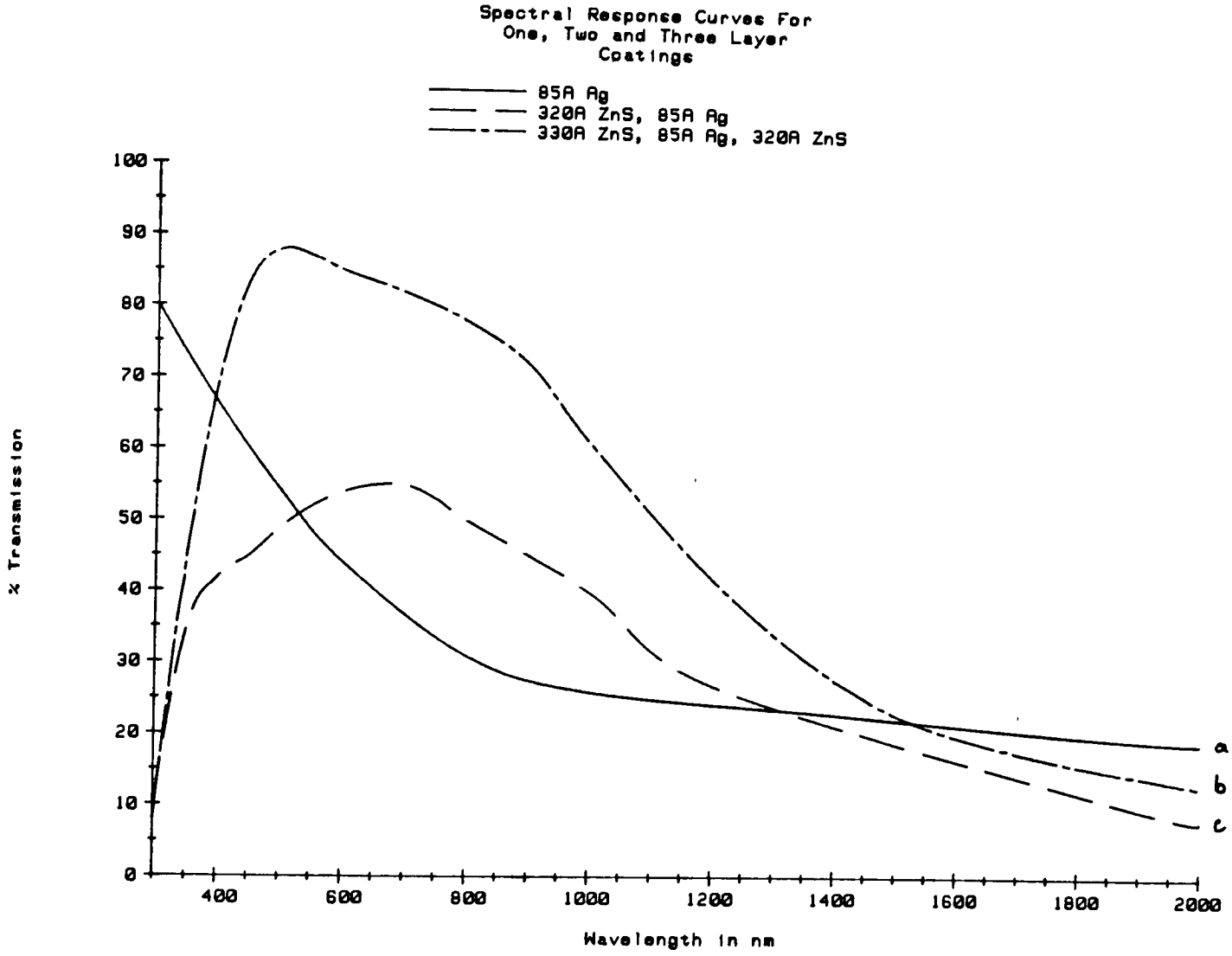
Spectral Response Curves For
One, Two and Three Layer
Coatings
85A Ag
320A ZnS, 85A Ag
330A ZnS, 85A Ag, 320A ZnS
% Transmission
100
90
80
70
60
50
40
30
20
10
0
400
600
800
1000
1200
1400
1600
1800
2000
Wavelength in nm
a
b
c

Figure 13

single and two-layer designs. Stability testing was performed on these filters.

Heat tests were performed on three-layer samples of 350Å ZnS/ 90Å Ag/ 350Å ZnS. Samples heated at 300°F for one hour showed no apparent degradation and transmission characteristics changed little. Samples heated at 500°F for one hour appeared light brown in color and reflection characteristics in the infrared region were destroyed. Figure 14 shows spectral characteristics for filters after heating at 300°F and 500°F for one hour compared to an untested filter. It is observed that the Ag/ZnS interface is not stable and interactions occur to destroy the transmission characteristics of the silver layer.

Computer optimizations of a five layer design with 20Å, 30Å, and 50Å of MgF_2 between ZnS and Ag layers are shown in Figure 15. Peak transmission is still above 80% at 500 nm, even when 50Å of MgF_2 is used. Based on previous experimental film thickness variations from design, MgF_2 thicknesses of 5Å, 10Å, and 20Å were coated between layers of ZnS (350Å) and Ag (90Å). Coating rates of the MgF_2 layers were kept low (around 2Å/S) due to thin film requirements. Spectral responses of these five-layer filters are shown in Figure 16. Only the 5Å MgF_2 sample shows response characteristics close to the three-layer design. Visible transmission is decreased considerably and a blue cast is apparent for 10Å and 20Å thicknesses.

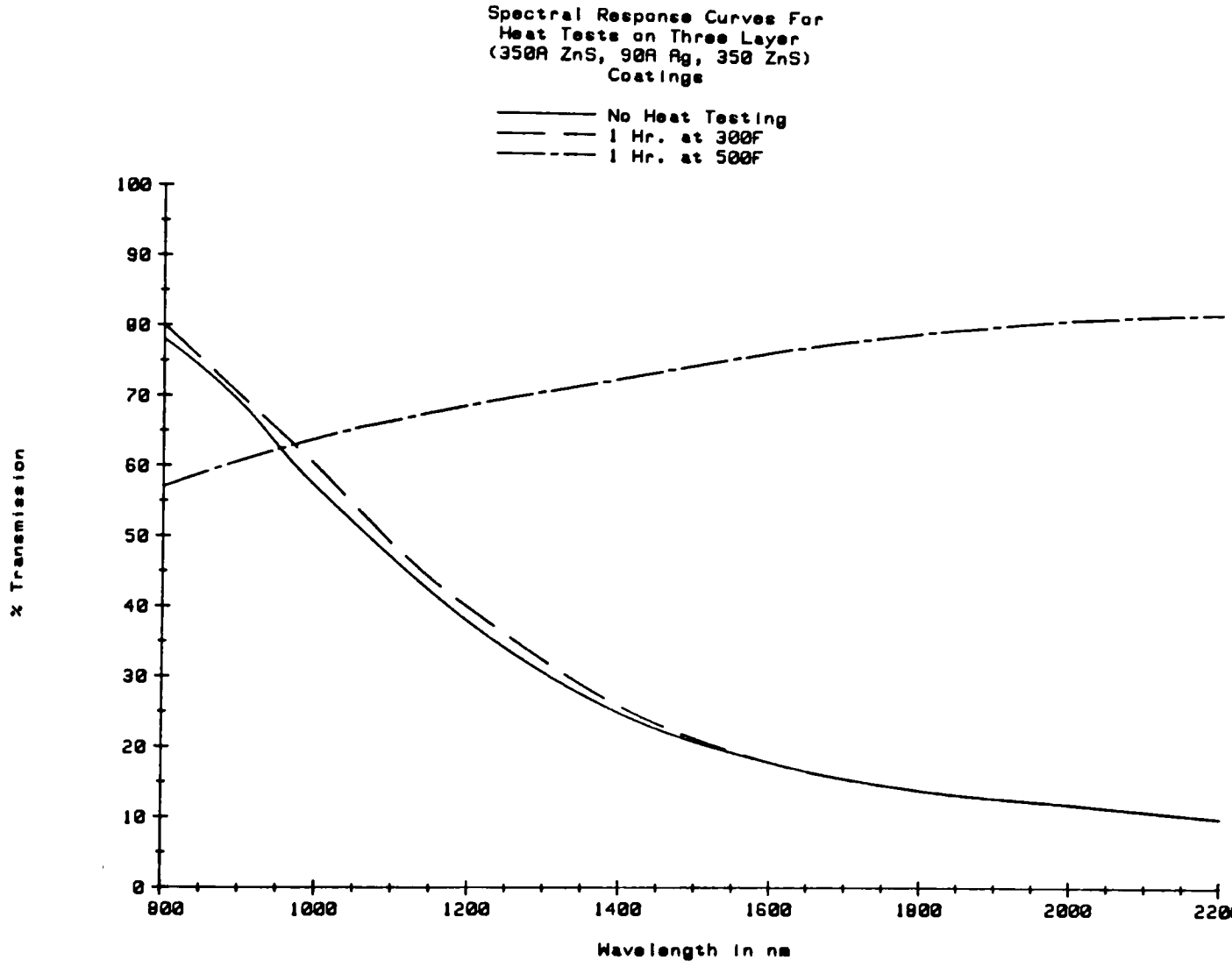
Spectral Response Curves For
Heat Tests on Three Layer
(350A ZnS, 90A Ag, 350 ZnS)
Coatings
No Heat Testing
1 Hr. at 300F
1 Hr. at 500F
% Transmission
100
90
80
70
60
50
40
30
20
10
0
800
1000
1200
1400
1600
1800
2000
2200
Wavelength in nm

Figure 14

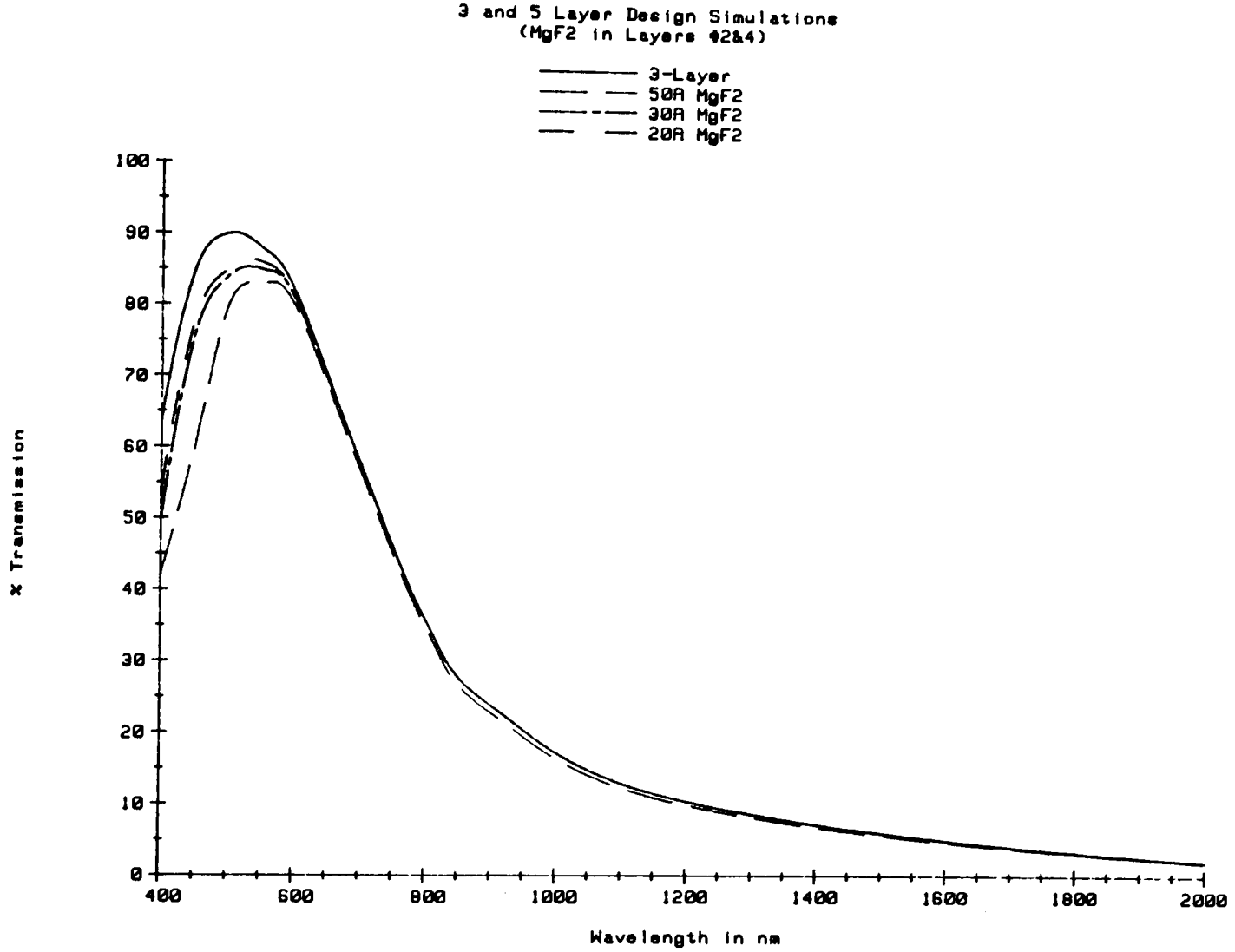
3 and 5 Layer Design Simulations
(MgF2 in Layers #2&4)
3-Layer
50A MgF2
30A MgF2
20A MgF2
% Transmission
100
90
80
70
60
50
40
30
20
10
0
400
600
800
1000
1200
1400
1600
1800
2000
Wavelength in nm

Figure 15

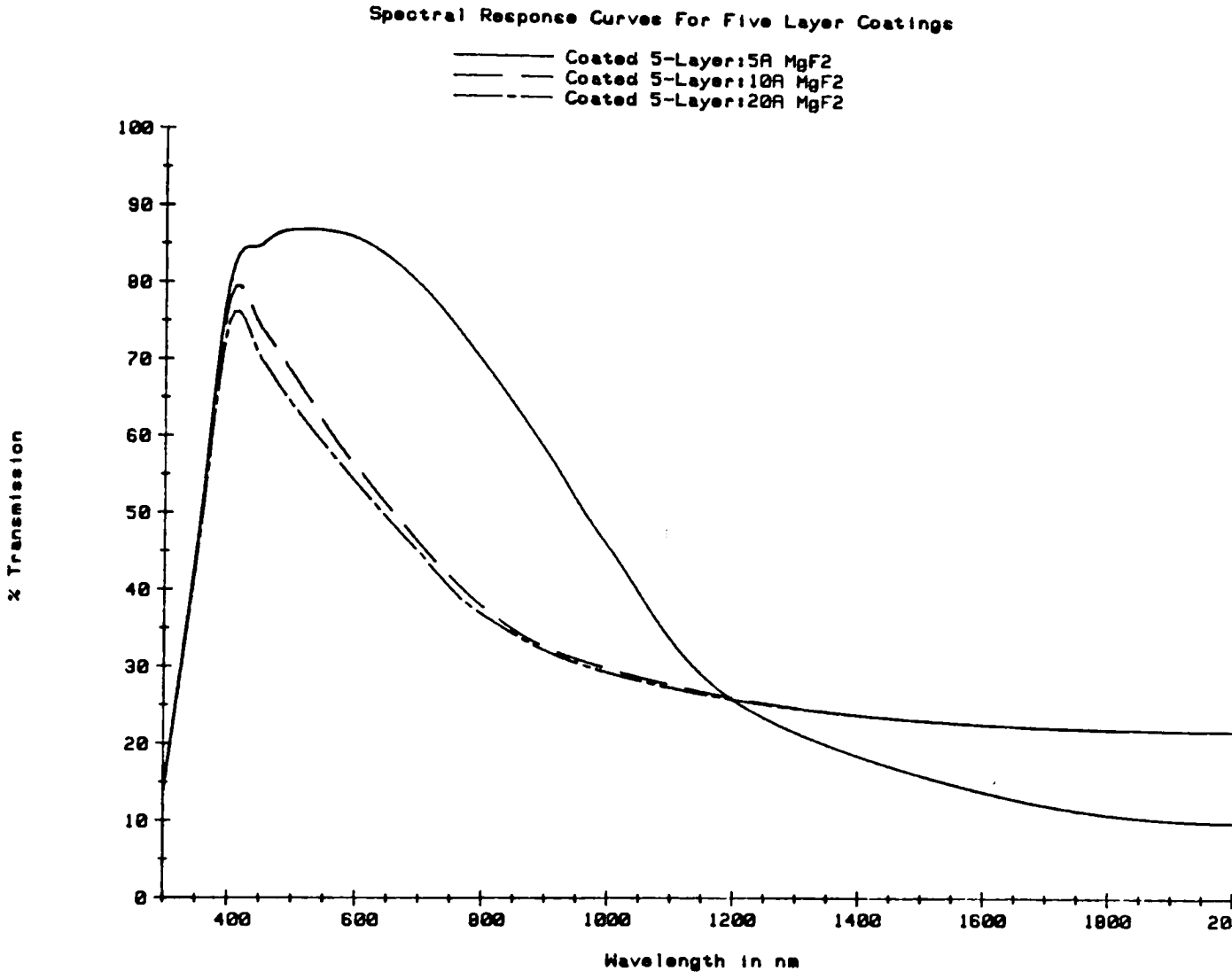
Spectral Response Curves For Five Layer Coatings
Coated 5-Layer:5A MgF2
Coated 5-Layer:10A MgF2
Coated 5-Layer:20A MgF2
% Transmission
100
90
80
70
60
50
40
30
20
10
0
400
600
800
1000
1200
1400
1600
1800
200
Wavelength in nm

Figure 16

Heat tests were performed with these five-layer filters as with the three-layer designs. A 300°F treatment for one hour changed characteristics of any filter little but a 500°F treatment destroyed IR reflection characteristics in all filters, turning them light brown in color. Figure 17 shows results of this testing. It was evident that these MgF_2 layers had no effect on increasing the stability of a Ag/ZnS filter system.

Investigation into any MgF_2/Ag interactions proved negative. An 80Å film of MgF_2 was coated on 100Å, 150Å, and 250Å samples of Ag to determine if it somehow depleted the metal layer. Heating at 400° and 500°F for one hour did not change the characteristics of these films. Spectral responses before and after heating for the thinnest (100Å) Ag film are shown in Figure 18.

It became evident that the MgF_2 had been incapable of isolating the ZnS from the Ag. The ZnS continued to deplete the Ag layer, even in the presence of the MgF_2 barrier. Barriers were either discontinuous or were made discontinuous by heating. Two possible solutions to this problem were incorporated into further barrier layer coatings. Thicker layers of MgF_2 (30Å and 40Å) were coated between layers of the ZnS/Ag/ZnS design (90Å Ag between two 800Å ZnS layers) at higher deposition rates (12-20Å/S). This produced filters with heat mirror characteristics better than those achieved previously with thinner MgF_2

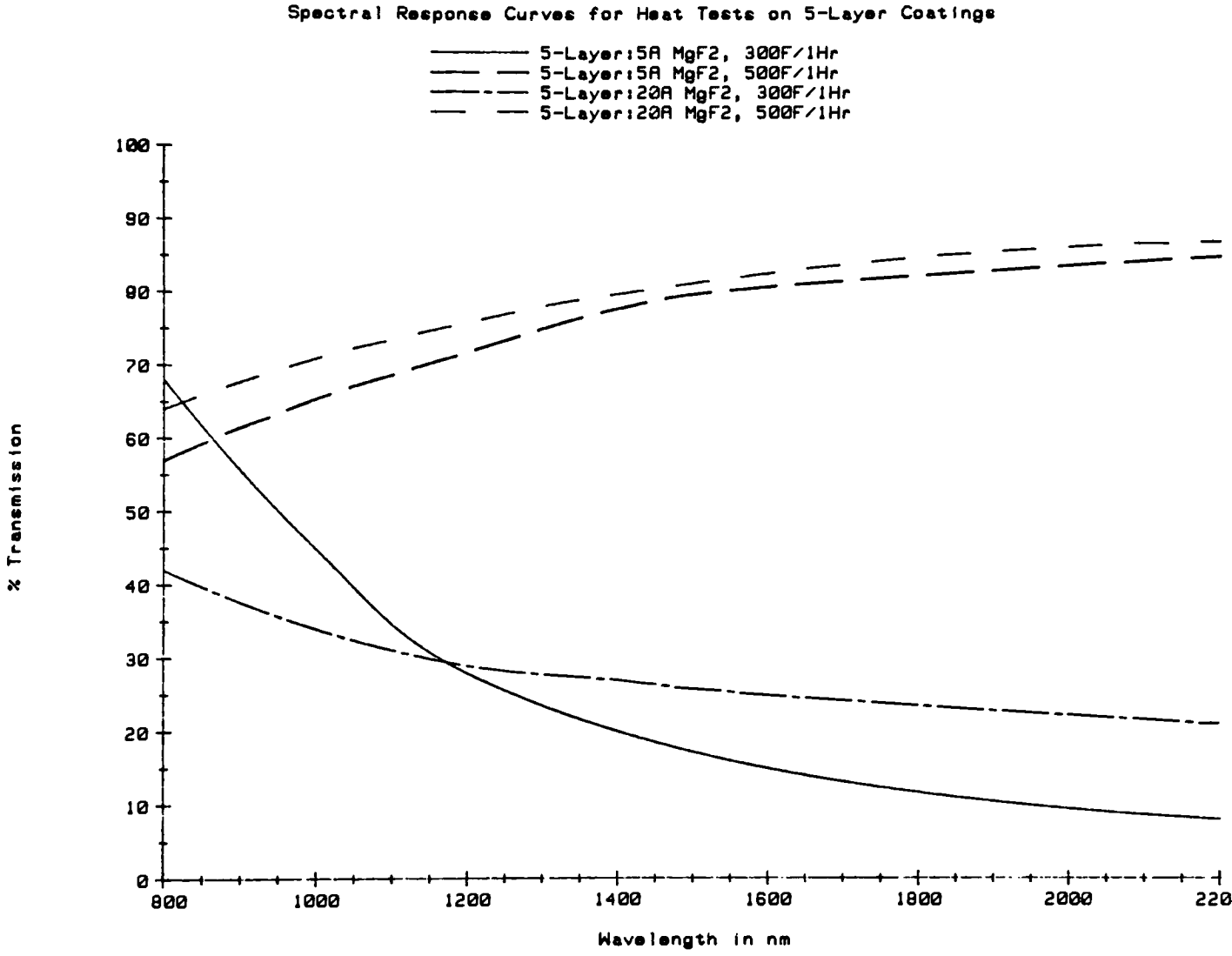
Spectral Response Curves for Heat Tests on 5-Layer Coatings
5-Layer:5A MgF2, 300F/1Hr
5-Layer:5A MgF2, 500F/1Hr
5-Layer:20A MgF2, 300F/1Hr
5-Layer:20A MgF2, 500F/1Hr
% Transmission
100
90
80
70
60
50
40
30
20
10
0
800
1000
1200
1400
1600
1800
2000
2200
Wavelength in nm

Figure 17

Spectrel Response of 85A MgF2 / 100A Ag / 85A MgF2
Before and After Heat Testing

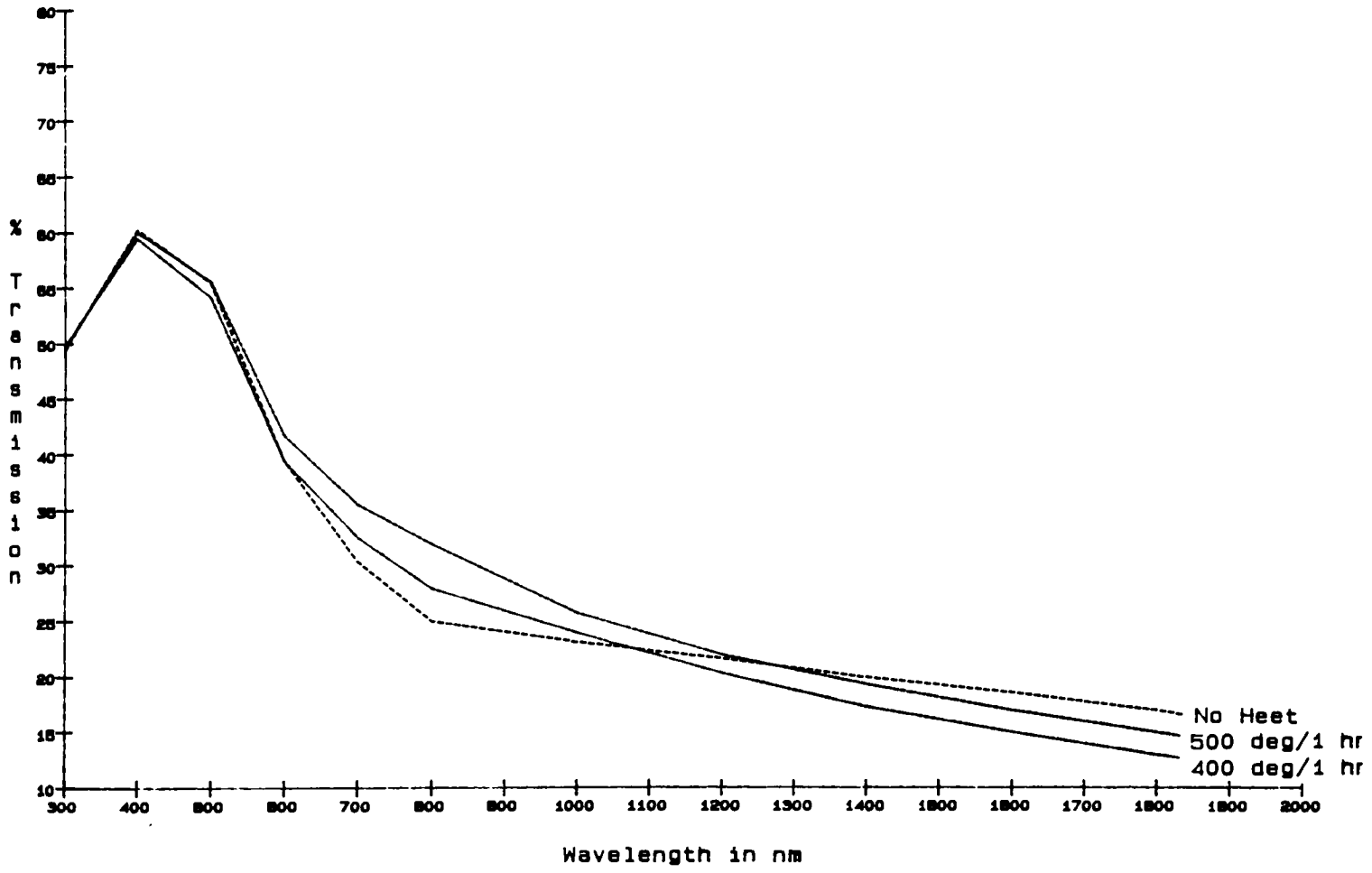

Figure 18

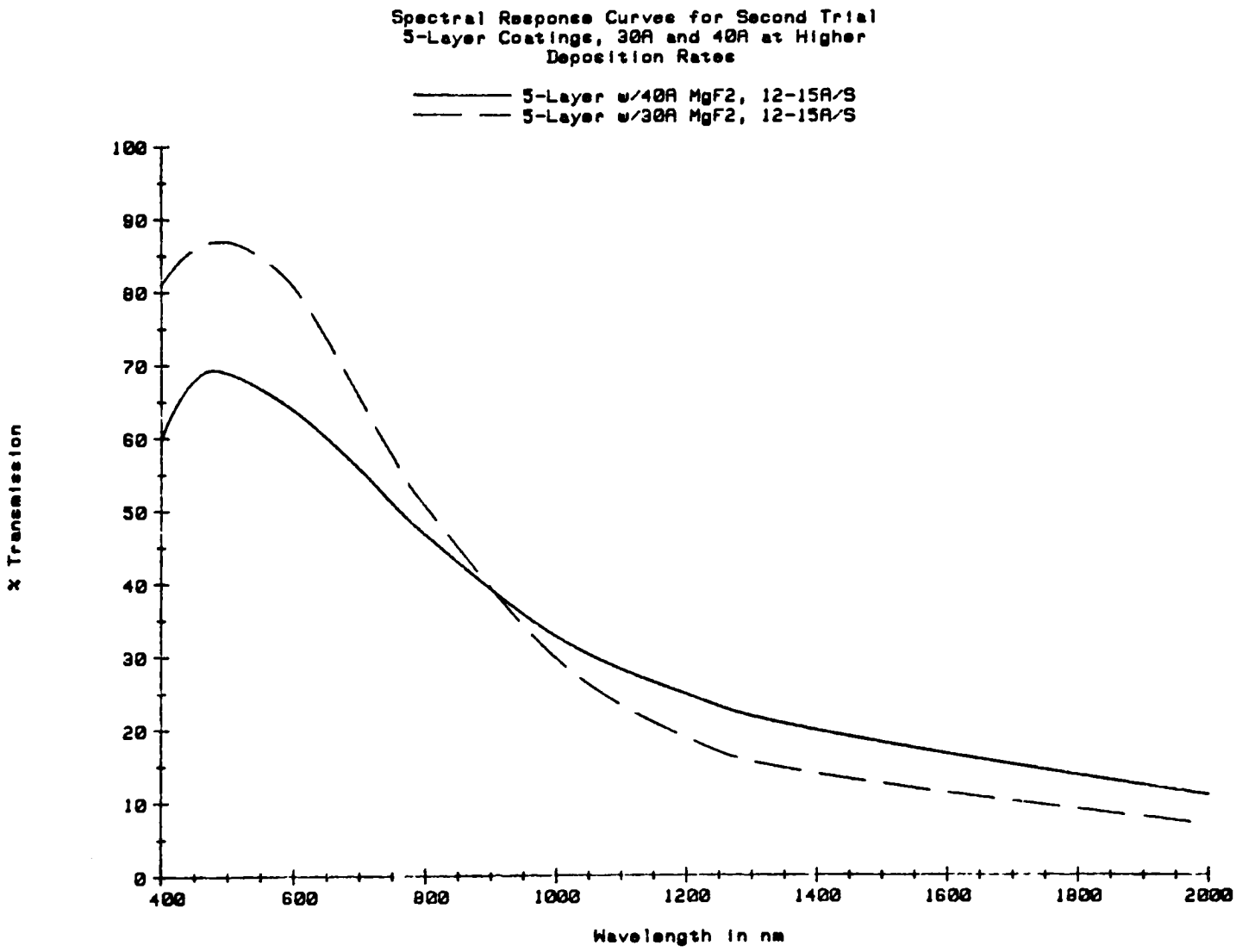
Spectral Response Curves for Second Trial
5-Layer Coatings, 30A and 40A at Higher
Deposition Rates
5-Layer w/40A MgF2, 12-15A/S
5-Layer w/30A MgF2, 12-15A/S
% Transmission
100
90
80
70
60
50
40
30
20
10
0
400
600
800
1000
1200
1400
1600
1800
2000
Wavelength in nm

Figure 19

layers (Figure 19). Films appeared slightly blue, but visible transmission remained high. The incorporation of the MgF_2 had given the filter a cutoff closer to the visible than the three-layer films.

Filters incorporated with both 30Å and 40Å of MgF_2 were heat tested for one hour at 400°, 500°, 600°, 700°, and 800°F. Filters with 30Å MgF_2 showed no appreciable optical changes at 400°F but decreased visible transmission and IR reflection occurred with 500°, 600°, and 700°F treatments. Filters treated at 700°F started to show signs of browning at the edges, attributed to non-uniform coating and thinner MgF_2 thicknesses outside of the center coating area. Although some optical degradation occurred, filters treated at these temperatures did retain good heat mirror characteristics. Filters treated at 800°F turned brown overall and optical characteristics deteriorated completely. Spectral characteristics are shown in Figure 20. Filters with 40Å barrier layers showed better resistance to heat treatment at 400°, 500°, and 600°F, showing no degradation at these temperatures. 700°F tests lowered visible transmission and IR reflection slightly and 800°F degraded filters completely. Figure 21 shows these results. Reflectance changes at 2000 nm from initial untreated values for both filter types at each treatment condition are shown in Table 2.

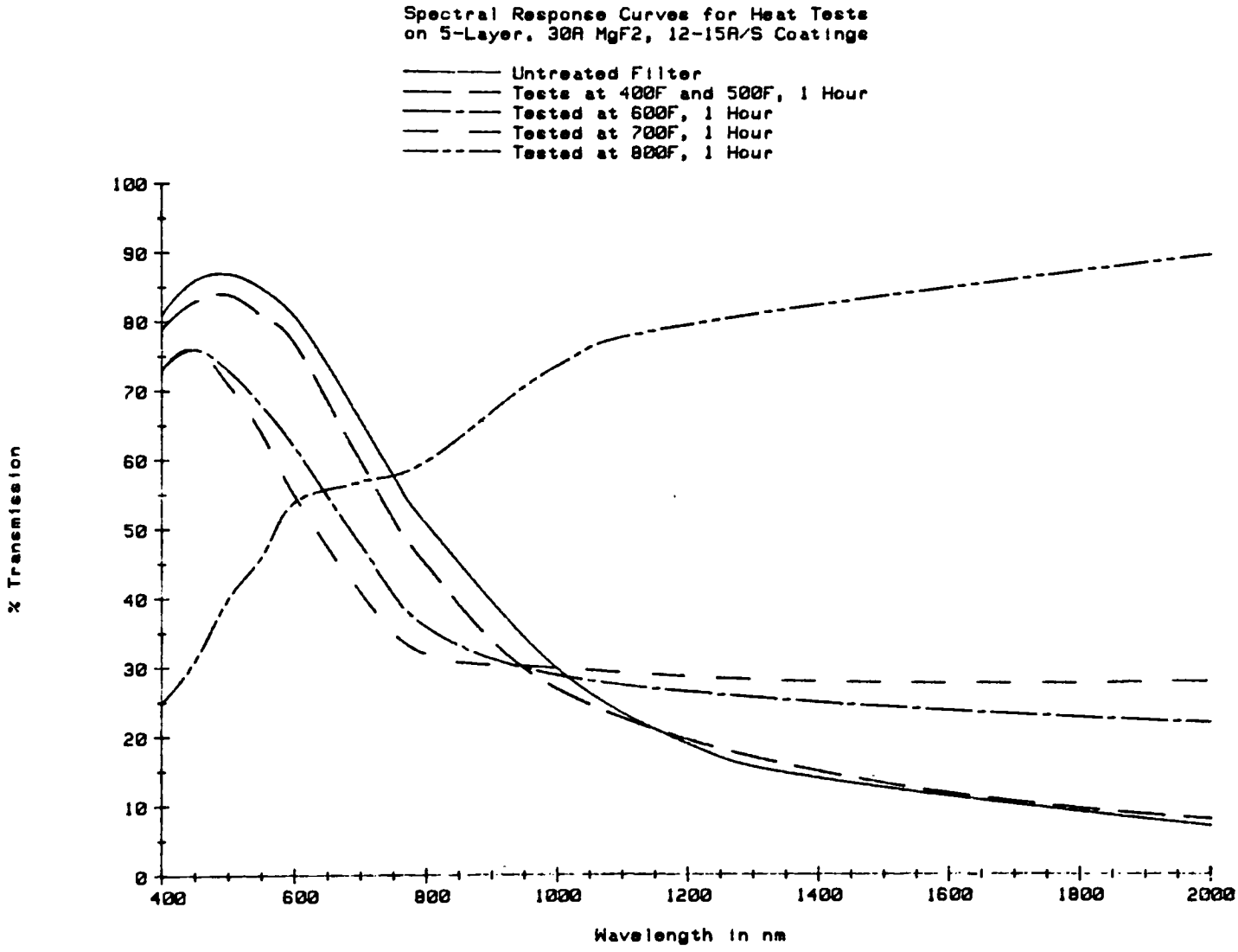
Spectral Response Curves for Heat Tests
on 5-Layer, 30A MgF2, 12-15A/S Coatings
Untreated Filter
Tests at 400F and 500F, 1 Hour
Tested at 600F, 1 Hour
Tested at 700F, 1 Hour
Tested at 800F, 1 Hour
% Transmission
100
90
80
70
60
50
40
30
20
10
0
400
600
800
1000
1200
1400
1600
1800
2000
Wavelength in nm

Figure 20

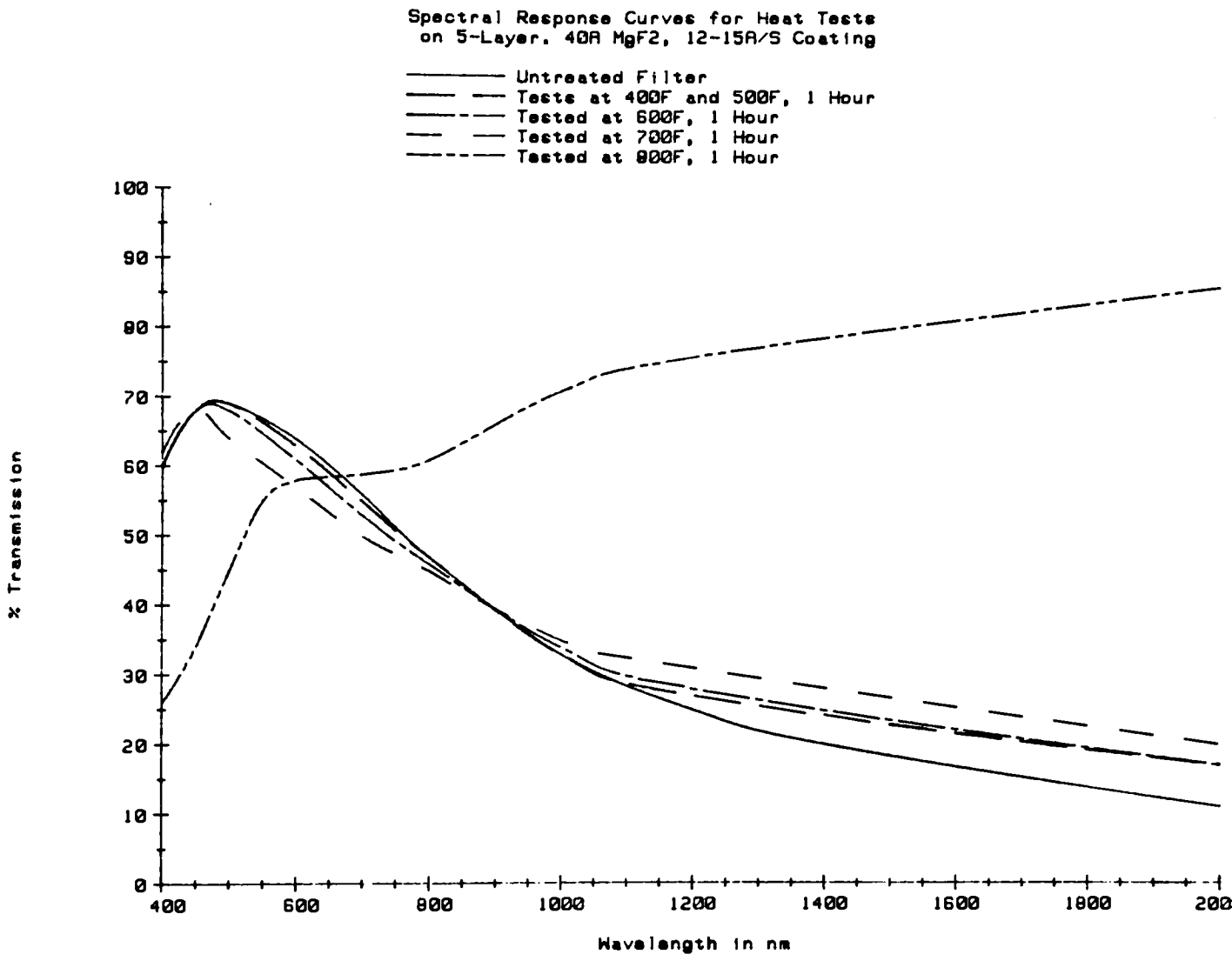
Spectral Response Curves for Heat Tests
on 5-Layer, 40A MgF2, 12-15A/S Coating
Untreated Filter
Tests at 400F and 500F, 1 Hour
Tested at 600F, 1 Hour
Tested at 700F, 1 Hour
Tested at 800F, 1 Hour
% Transmission
100
90
80
70
60
50
40
30
20
10
0
400
600
800
1000
1200
1400
1600
1800
2000
Wavelength in nm

Figure 21

TABLE 2

Reflectance Changes at 2000 nm for Heat Tested Filters

Filter/ Treatment	% Reflectance Loss at 2000 nm
5 Layer w/30 A MgF2	
500 degrees F/1 hr	2%
600	15
700	21
800	83
5 Layer w/40 A MgF2	
500	6%
600	6
700	9
800	74

Discussion

Optical and structural properties of thin metal films are dependant on the conditions by which they are deposited. Thin film properties are influenced by surface and impurity effects and are, therefore, different from bulk metal properties. The spectral absorption equations used for theoretical calculations are for pure metals. Impurity defects and the existence of oxides provide sources of absorption and scattering, resulting in deviations from expected responses. In Figure 22, the experimental 85Å Ag film is plotted along with calculated transmission values for a 100Å Ag film on glass. Additionally, reflection and absorption values are calculated and are contained in Appendix III. Transmission of the experimental film deviates from the theoretical curve. These deviations can be attributed to nucleation effects, impurity concentrations, thin film properfties, and deposition conditions.

Structural properties of thin metal films are influenced by deposition rate, angle, and energy as well as the substrate type and condition [Vossen, 1977]. Although experimental silver films were deposited onto glass substrates at room temperature to minimize migration and agglomeration (which would lead to scattering), large island formation is not completely preventable in metal on glass

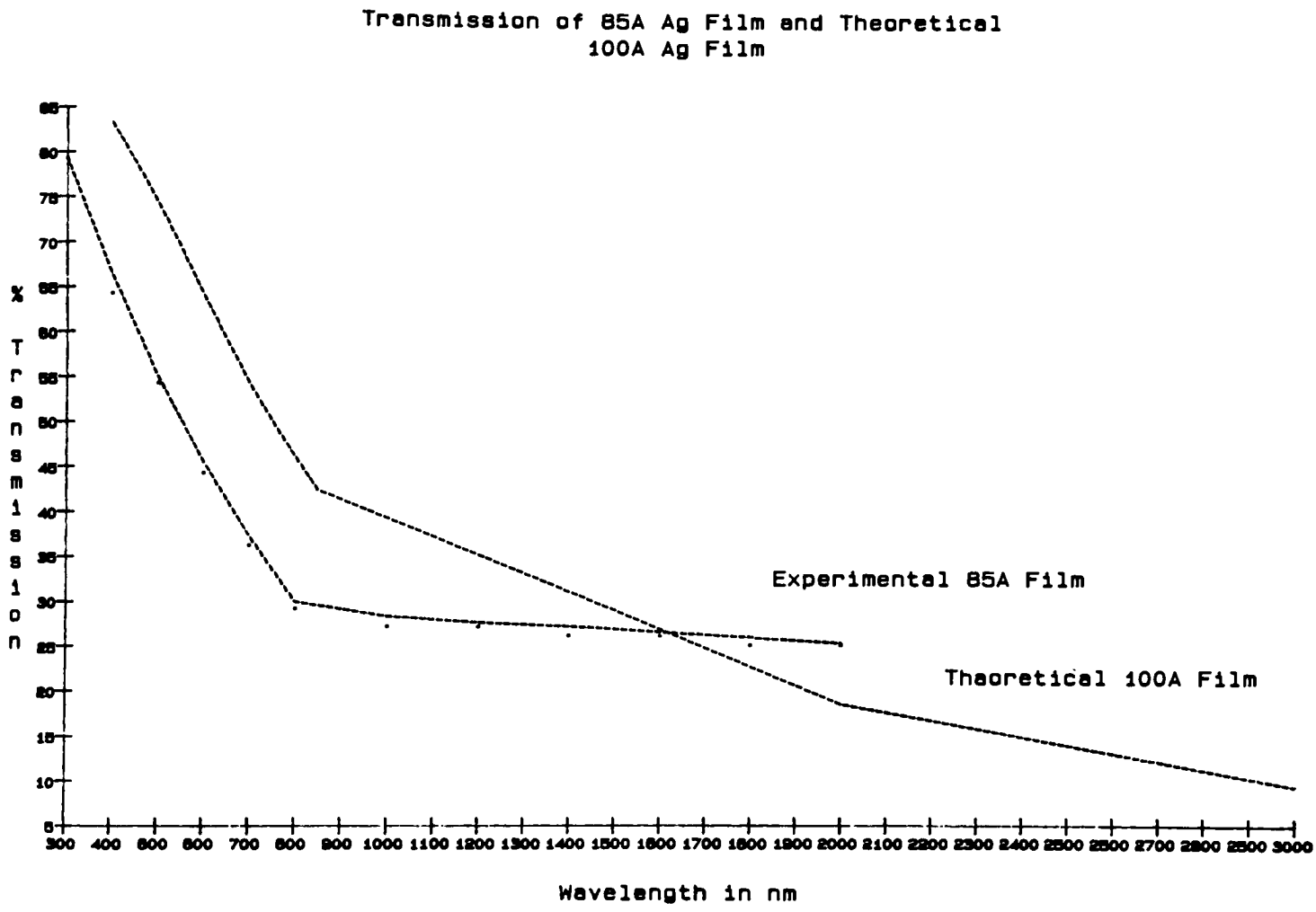
Transmission of 85A Ag Film and Theoretical
100A Ag Film
% Transmission
Experimental 85A Film
Theoretical 100A Film
Wavelength in nm

Figure 22

depositions.

The growth of metal films on an insulator (i.e. glass) occurs in an "island-nucleation" mode, known as a Volmer-Weber mode [Venables, Spiller, Hanbucken, 1984]. Metal atoms are more strongly bound to like atoms than they are to the glass substrate, tending toward large island formation upon condensation. Additionally, substrate surfaces introduce defects and impurities which will alter the condensation of the metal. If the binding energy at point locations on the substrate is large, nucleation sites are possible and large island growth becomes more substantial. Condensation at the sites may also re-arrange to form impurity compounds or other defects, allowing additional scattering and absorption effects.

High vapor flux density of the arriving metal atoms and large kinetic energies will result in large island formation, imparting momentum and energy sufficient for lateral mobility and combination at nucleation or point defect sites. Deposition maintained at a low rate (<20Å/sec) produces a low arriving flux density, minimizing migration. At extremely low rates, the possibility for substantial introduction of impurities exists during condensation, causing additional transmission losses due to scattering. Normal incidence of deposition also decreases possibilities for agglomeration. Increasing deposition angle provides a higher lateral momentum to the vapor,

increasing mobility and allowing island formation at nucleation sites.

Ideally, the absence of agglomeration, or island formation, is desired in a thin film, but absorption and scattering effects cannot be completely controlled or eliminated in a deposition process. The means by which a material is deposited determines its composition, its structure, and its surface morphology. In addition to arriving vapor and substrate thermal effects, electrostatics effects contribute to agglomeration and coalescence.

Electrical charge contribution and vapor kinetic energy introduced by a process will play a large role in the structure and composition of a thin film. Deposition through sputtering, resistive evaporation, and electron beam evaporation introduce differences in electrical effects. With resistive evaporation, electrical charge differences between the vapor and the substrate exist which affect island size and spacing. Silver vapor possesses a negative charge [Kasprak, et al, 1974] and will repel a negatively charged substrate, resulting in increased mobility, greater potential for large island formation through trapping at defect sites, and increased scattering. The opposite effect will occur if the substrate is positively charged. This scattering could be reduced, therefore, if a dc electric field were placed at the substrate, causing silver ions to be trapped immediately by the substrate.

Imourity concentration affects transmission of thin films. The theoretical soectral response is for pure silver and. as noted previously, high impurity concentration is likely in thin metal films and increases scattering. Impurities in metal films will also reduce conductivity. Electrons going through collisions convert energy to heat and increase absorption. The effect of impurities on conductivity becomes more pronounced if the valence of the impurity differs greatly from the metal. Oxides of metals can decrease conductivity (and increase absorbance) substantially.

Surface scattering occurs from surface roughness characteristics of metal films. Any large island formation increases roughness at the surface of a film. As light falls onto a film surface, it is reflected diffusely and specularly. The ratio of specular reflection (or scattering) R, to reflection at a smooth surface, R_o, shows the effects of surface roughness on transmission characteristics:

$$R/R_o = \exp[-(4\pi r/\lambda)^2] + [1-\exp[-(4\pi r/\lambda)^2]][1-\exp[-2(\pi a/m\lambda)^2]] \qquad (3)$$

where r is RMS surface roughness, m is RMS slope of irregularities, and a is the half-acceptance angle of the measuring device [Vossen, 1977]. From this equation, it

is apparent that scattering effects due to surface roughness becomes more pronounced with decreasing wavelength. Transmission at visible wavelengths can be substantially decreased through surface scattering of a metal film.

Reflection in the infrared and transmission in the visible by thin silver films show them to exhibit heat mirror characteristics, though heat reduction and visible transparency capabilities would be inadequate for applications with tungsten light sources. Using a light-to-heat ratio:

$$L/H = \frac{average\ T(vis)}{average\ T(long)} \qquad (4).$$

where *average T(vis)* is the average visible transmission from 380 nm to 760 nm and *average T(long)* is the average IR transmission from 760 nm to 2700 nm, heat mirror capabilities can be defined. The single layer silver film as shown in Figure 22 has a 1.7:1 L/H ratio. Although infrared reflection is approximately 80%, average visible transmission of only around 50% is achieved.

Silver layers applied over a zinc sulfide layer possess higher transmission than silver applied directly over glass. Average visible transmission is raised to over 60%. This increase in transmission is partially due to a decrease in absorption characteristics of the silver layer when applied over the dielectric material. Holland and

Siddel [1958] reported that conductivity of thin metal films applied over a layer of metal oxide was higher than conductivity of metal films over glass. Higher conductivity in metal films results in decreased absorption.

Any structural changes in the silver layer when coated over zinc sulfide would affect conduction and absorption characteristics. If zinc sulfide altered island formation during silver condensation, agglomeration might be reduced along with absorption and scattering effects. The "nucleation-modification" has been observed with several materials under metal layers, including semiconductor compounds, adsorbed oxygen, and other metals [Gillham and Preston, 1955] [Vossen, 1977]. This effect probably occurs due to the abundance of point defects (possibly charged) in an amorphous layer of zinc sulfide, as compared to a glass surface. These defects prevent large island formation by allowing many possible sites for growth. Additionally, during resistive evaporation, electron emission occurs as material is evaporated, which can subsequently charge the substrate. After deposition of the zinc sulfide layer, a uniformly charged surface exists on the substrate, reducing individual charge sites for possible metal ion trapping and island formation.

ZnS coating beneath Ag films increase transmission through optical interference effects (equation 2). The thickness of the ZnS is not the conventional quarter

wavelength of 570Å at 550 nm, but rather 320Å (.147 wavelength). This occurs because the refractive indices of ZnS are higher than those of Ag.

A conventional quarter wavelength film provides increased transmission through destructive interference at its surfaces. For light at normal incidence, reflections from the second surface of a film is one half wavelength out of phase with light reflected from the first surface. The destructive interference which occurs from the cancellation of reflections from these two surfaces allows total transmission of all energy incident on the surface. ZnS at the bottom surface provides a low reflective coating for the silver-glass separation. A ZnS layer of this type coated over a silver film also produces low reflection situations at silver-air separations.

The reduction in visible reflectance obtained with the ZnS bottom layer decreases absorption and scattering characteristics of the silver film. An increase in light-to-heat production ratio by 35% to 2.3:1 occurs.

The effectiveness of the Ag/ZnS heat mirror was increased further with the incorporation of a ZnS top layer, coated over the silver, equal in thickness to the ZnS bottom layer (Figure 13c). Light-to-heat production is increased to 3.5:1, with an average visible transmission of 80%. Optical properties of the glass substrate contribute somewhat to the transmission loss of the system. Absorption

in glass is near 6% and cannot be decreased any with optical coating methods [Yoldas, 1984]. A transmission of 87% at 550 nm, therefore, represents a loss of 7% transmission from the coating itself. Since ZnS films are essentially non-absorbing, infrared reflectivity of the underlying silver film is not affected. The three layer coating obtained, where transmission is induced in a silver film by dielectric coatings, represents optimization for the the human spectral response, with a peak sensitivity at 550 nm (Figure 7).

The peak IR reflection area for an ideal system should be near 900-1200 nm, corresponding to a maximum output of a tungsten source (Figure 6). Transmission near 60% is obtained in this region. insufficient to reduce heat production completely at near infrared wavelengths. Infrared reflectivity is near 80% at wavelengths beyond 1200 nm, decreasing energy loss due to mid and far infrared production. Figure 23 shows the product of the three layer filter and a 2500K tungsten source. The values demonstrate the normalized output of a tungsten / heat mirror system at wavelengths from 400-3000 nm. The system output is plotted against a normalized tungsten source for comparison. As seen, the peak output shifts from 1100 nm to 900 nm, changing visible transmission little but substantially decreasing infrared transmission.

The usefulness of the ZnS/Ag/ZnS films in lighting

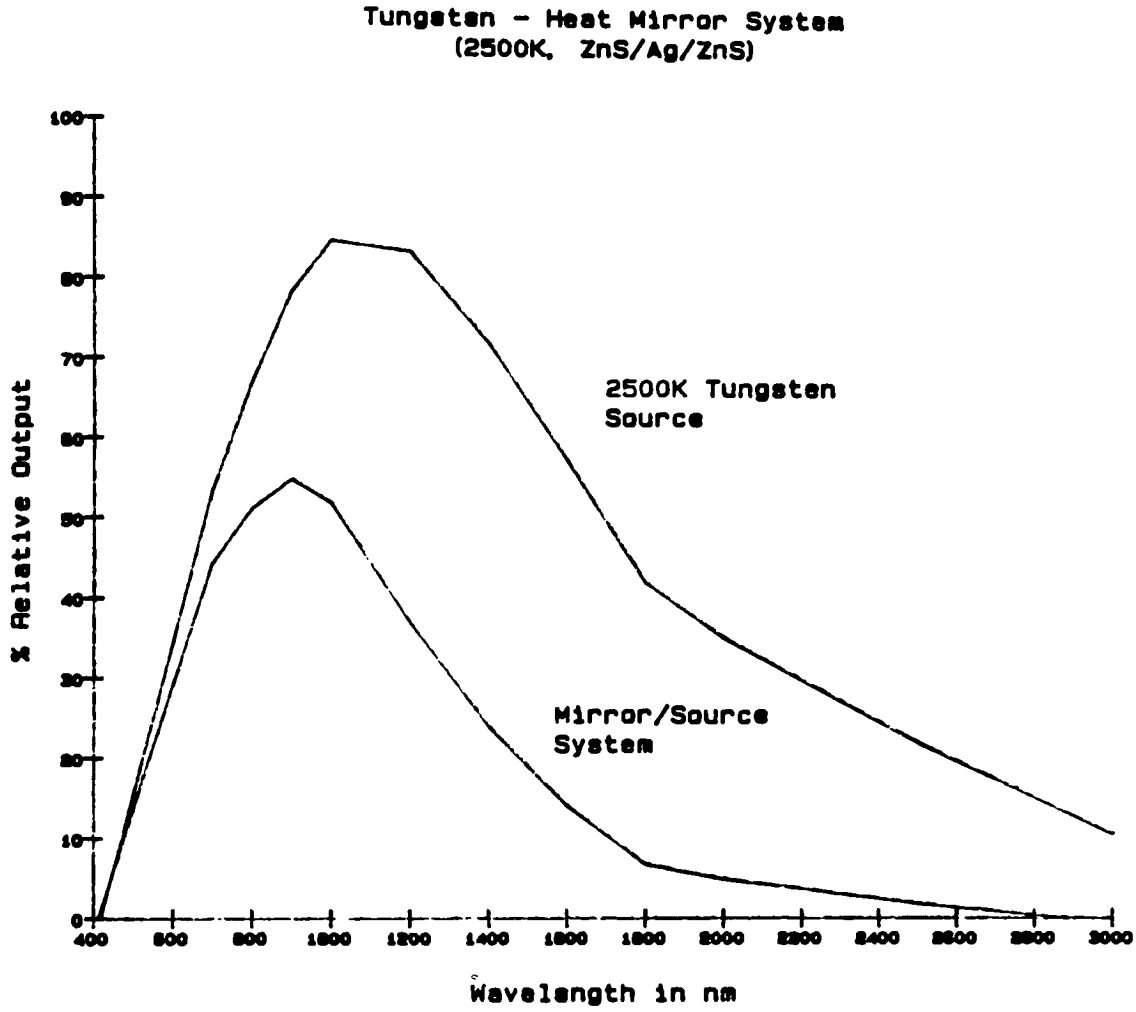
Tungsten - Heat Mirror System
(2500K, ZnS/Ag/ZnS)
% Relative Output
100
90
80
70
60
50
40
30
20
10
0
2500K Tungsten
Source
Mirror/Source
System
400
800
1200
1400
1600
1800
2000
2200
2400
2600
2800
3000
Wavelength in nm

Figure 23

applications will depend on their stability under operating conditions. Although no degradation occurred to the filters heated to 300° F for one hour, substantial changes in heat mirror performance occurring with treatment at 500° F for one hour show these filters to be unstable in moderately high temperature conditions. This irreversible optical degradation with heating renders the filters inadequate for use with tungsten light sources, despite their good initial spectral characteristics.

Operation of the filters under the vacuum environment of a tungsten lamp would isolate the coating from the environmental effects (such as humidity) which may contribute to instability. Additionally, a protective transparent coating over the filters may provide some isolation [Koltun, et al, 1975]. Incorporation of a thin MgF2 barrier layer between the ZnS and Ag layers was chosen for investigation to inhibit chemical reaction and improve stability of the filters.

From Figure 20, L/H ratio of the five layer designs with 30Å MgF_2 approximately equal to is the three layer value of 3.5:1 and maintains a large value during heat testing up to 700° F. Incorporation of 30 to 40Å of MgF_2 at deposition rates of 12 to 20 Å/sec resulted in better heat mirror characteristics and higher temperature stability than filters produced with 5 to 20Å MgF_2 at 2 to 5 Å/sec. The mechanics causing this phenomena is likely the continuity of

the MgF_2 film over Ag.

Actual films of MgF_2, Ag, and ZnS are not homogeneous at interfaces; they are not smooth or well defined. The transition regions may be large compared to optical thicknesses and may provide substantial changes in characteristics of filter combinations. The study conducted with thin MgF_2 films over various thicknesses of Ag films showed contribution by transition areas between these two films to be negligible. Discontinuity of MgF_2 layers instead produces inadequate isolation of Ag and ZnS layers.

Rate control during deposition is important for optical films [Thermionics] and a heated substrate is often required. During film growth at extremely low rates, high impurity contribution is likely, resulting in agglomeration and discontinuity. Films substantially different from pure MgF_2 form, accounting for deviations in optical characteristics. The incorporation of a barrier layer of MgF_2 of appropriate thickness provides protection from interaction between Ag and ZnS films at temperatures up to 700° F.

Conclusion

Transparent heat mirrors have been produced from a transmission induced thin metal film, utilizing silver and zinc sulfide. Filters exhibit 87% peak transmission while reflecting 80% in the infrared. Thin film optical properties are influenced greatly by deposition conditions, nucleation effects, and impurities. It has been shown that the zinc sulfide serves as a nucleation modifying layer during silver film growth, allowing continuous film growth with reduced agglomeration, as well as an optical interference film for increased visible transmission. Although these heat mirrors have poor thermal and chemical stability, the incorporation of thin barrier layers of magnesium fluoride provide isolation and stability up to 700° F. Film growth rates high enough to minimize impurity effects is required, with films thick enough to provide continuity.

The stability of these filters under incandescent operating conditions is uncertain, although their use under vacuum conditions in the absence of moisture would improve performance. The dielectric / metal / dielectric system is more economical to produce than an all dielectric filter, but the success of a energy efficient incandescent lamp involves more than producing a suitable coating. Lamp envelope coating and filament considerations have to be

addressed further. Coating over flat substrates is not representative of the difficulties involved with coating the interior of a curved lamp. Additionally, filament operating temperature will be affected during operation with a heat mirror coating. This study has produced filters with heat mirror characteristics suitable for incandescent lighting applications. Optimization of these applications need further investigation.

References

American Institute of Physics Handbook(AIP), 3rd Edition, 6-137, 1972.

Agnihotri, O.P; Sharma, A.K.; Gupta, B.K.; and Thangaraj, R., "The Effect of Tin Additions on Indium Oxide Selective Coatings", J. Phys. D: Appl. Phys., 22, 643, (1978).

CRC Handbook of Chemistry and Physics, 65th Edition, CRC Press, New York, 1984.

Fan, J.C; Bachner, F.J.; Foley, G.H.; and Zavracky, P.M, "Transparent Heat Mirror Films for Solar Energy Collection", Appl. Phys. Lett., 25, 693, (1974).

Fan, J.C. and Bachner, F.J., "Transparent Heat Mirrors for Solar Energy Applications", Appl. Opt., 15, 1012, (1976).

Fan; J.C.; Bachner, F.J.; and Murphy, R.A., "Thin-Film Conducting Microgrids as Transparent Heat Mirrors", Appl. Phys. Lett., 28, 440, (1976).

Glaser, H.J., Proceedings, Eighth International Vacuum Congress, 1, 723, (1980).

Granqvist, C.G., "Radiative Heating and Cooling with Spectrally Selective Surfaces", Appl. Opt., 20, 2606, (1981).

Granqvist, C.G. and Hamberg, I.H., "Band-Gap Widening in Heavily Sn Doped In_2O_3", Phys. Rev. B, 30, 3240, (1984).

Groth, R. and Kauer, E., Philips Tech. Rev., 26, 105, (1965).

Hamberg, I.; Hjortsberg, A.; and Granqvist, C.G, "High Quality Transparent Heat Reflectors of Reactively Evaporated Indium Tin Oxide", Appl. Phys. Lett., 40, 362, (1982).

Hass, G., "Mirror Coatings for Low Visible and High Infrared Reflectance", JOSA, 46, 31, (1956).

Holland, L. and Siddall, G., "Heat-Reflecting Windows Usind Gold and Bismuth Oxide Films", Brit. J. Appl. Phys., 9, 359, (1958).

Jarvinen, P.O., "Heat Mirrored Solar Energy Receivers", J. Energy, 2, 95, (1978).

Koltun, M.M.; Gaziev, U. Kh.; and Faiziev, Sh. A., "Investigation of Glass and Polymer Insulation with Transparent Heat Reflecting Coatings for Solar Installations", Geliotekhnika [Applied Solar Energy], 11, 32, (1975).

Liddell, H.M., Computer Techniques for the Design of Multilayer Filters, Adam Hilger Ltd., Bristol, G.B., 1981.

Macleod, H.A., Thin Film Optical Filters, American Elsevier, New York, 1969.

Smith, W.J.,Modern Optical Engineering, McGraw-Hill, New York, 1966.

Stimson, A.,Photometry and Radiometry for Engineers, Wiley, New York, 1974.

Thelen, A.,"Multilayer Filters with Wide Transmittance Bands, JOSA, 53, 253. (1963).

Thermionic Vacuum Products, Evaporation Tables.

Venables, V.A.; Spiller, G.T.D.; and Hanbucken, M., "Nucleation and Growth af Thin Films", Rep. Prog. Phys., 47, 399, (1984).

Yoldas, B.E. and O'Keefe, T., "Deposition of Optically Transparent IR Reflective Coatings on Glass", Appl. Opt., 23, 3638, (1984).

Vossen, J.L., Transpearent Conducting Films", Phys. Thin Films, 9, (1977).

Apoendix I

Optical characteristics in metal films are determined by two parameters called optical constants. One constant, the refractive index n, is the ratio of the phase velocitv of light in vacuum to the phase velocitv of light in the material. The second ootical constnt, the extinction coefficient k, corresponds to the exponential decav of a wave as it propagates through a material. The complex index of refraction combines these two optical constants into one:

$$N = n - ik. \qquad (1.1)$$

Despite the term, these parameters are not constant but strongly wavelength dependant. The effects of the refractive index and extinction coefficient on the reflective, transmittive, and absorptive characteristics of a metal depend on the configuration of the optical svstem.

In a situation where light is incident from air onto an absorbing metal film of thickness t, refractive index n, and extinction coefficient k coated on a weakly absorbing substrate of refractive index ns and extinction coefficient ks:

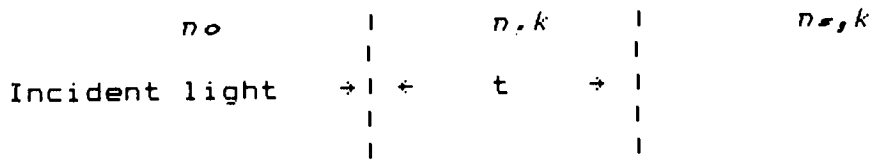

reflection R and transmission T of a normally incident wave can be calculated as follows [Hass and Hadley, 1963]:

$$R = \frac{a(1)e^{x}+a(2)e^{-x}+a(3)\cos(f)+a(4)\sin(f)}{b(1)e^{x}+b(2)e^{-x}+b(3)\cos(f)+b(4)\sin(f)} \quad (1.2)$$

$$T = \frac{16ns(n^2+k^2)}{b(1)e^{x}+b(2)e^{-x}+b(3)\cos(f)+b(4)\sin(f)} \quad (1.3)$$

where:

$$a(1) = [(1-n)^2+k^2][(n+ns)^2+(k+ks)^2]$$
$$a(2) = [(1+n)^2+k^2][(n-ns)^2+(k-ks)^2]$$
$$a(3) = 2[[1-(n^2+k^2)][(n^2+k^2)-(ns^2+ks^2)]+4k(nks-nsk)]$$
$$a(4) = 4[[1-(n^2+k^2)][(nks-nsk)-k[(n^2+k^2)-(ns^2+ks^2)]]$$

$$x = 4\pi kt / \lambda$$
$$f = 4\pi nt / \lambda$$

$$b(1) = [(1+n)^2+k^2][(n+ns)^2+(k+ks)^2]$$
$$b(2) = [(1-n)^2+k^2][(n-ns)^2+(k-ks)^2]$$
$$b(3) = 2[[1-(n^2+k^2)][(n^2+k^2)-(ns^2+ks^2)]-4k(nks-nsk)]$$
$$b(4) = 4[[1-(n^2+k^2)][(nks-nsk)-k[(n^2+k^2)+(ns^2+ks^2)]].$$

Reflection and transmission values must be calculated for each wavelength, with corresponding n and k values. Setting ks to zero for glass substrate (negligible absorbtion) makes computation easier. Total absorption can be calculated as:

$$A = 1 - T - R. \quad (1.4)$$

```
10 REM ***********************************
20 REM
25 REM    REFLECTANCE AND TRANSMITTANCE
28 REM  FOR NON-ABSORBING/NON-DISPERSIVE
30 REM             dLAYERS
35 REM
40 REM  B.W. SMITH 10/86 REF.H.M. LIDDELL
45 REM
47 REM ***********************************
50 DIM R(50),X(50),WAV(50),FRQ(50),REF(50),PR(50),SR(50).TS(50),PT(50).ST(50)
60 DIM CJ(50),Z(50),R1(50)
90 REM  INPUT DATA
100 REM  LAYER PARAMETERS   MAX=50
110 INPUT"TOTAL LAYERS":N
120 INPUT"N(A),N(S)";AIR,SUB
122 RA=AIR
124 RS=SUB
130 FOR I=1 TO N
140 INPUT"(N(I).T(I)) FOR EACH LAYER";R(I),X(I)
145 NEXT I
150 REM  SPECTRAL INFORMATION  MAX=50
155 INPUT"NUMBER OF WAVELENGTHS":M
160 INPUT"(REF,INITIAL,INCREMENT) WAVELENGTHS";RFW,WAV(1),INC
170 FRQ(1)=RFW/WAV(1)
180 FOR I=2 TO M
190 WAV(I)=WAV(I-1)+INC
200 FRQ(I)=RFW/WAV(I)
210 NEXT I
220 INPUT"ANGLE OF INCIDENCE (DEG)":A1
222 AN=A1
230 REM CALCULATION OF RESULTS
240 GOSUB 2000
245 OPEN4.4:CMD4
250 REM  PUT OF  RESULTS
260 PRINT"REFERENCE WAVE =  ";RFW
270 PRINT"N(AIR) =  ";AIR
280 PRINT"N(SUB) =  ";SUB
290 PRINT:
300 PRINT"LAYER PARAMETERS:":
310 PRINT"INDEX"."THICKNESS"
320 FOR I=1 TO N
330 PRINT R(I),X(I)
340 NEXT I
350 PRINT::
360 PRINT"FOR THIS ":N;" LAYER FILTER, AT AN ANGLE OF INCIDENCE = ";AI;" DEG
370 PRINT:
375 PRINT"RELECTION:":
380 PRINT"WAVELENGTH","P-COM","S-COM"."AVG REFL"
385 FOR I=1 TO  M
390 PRINT WAV(I),PR(I),SR(I).REF(I)
400 NEXT I
```

```
410 PRINT:
420 PRINT"TRANSMISSION:":
430 PRINT"WAVELENGTH","P-COM","S-COM","AVG TRANS"
440 FOR I=1 TO M
450 PRINT WAV(I),PT(I),ST(I),TS(I)
460 NEXT I
490 CLOSE 4
500 END
2000 REM  EVALUATION SUBRINE
2005 TBS=0
2010 THT=/180*AN
2020 SH=SIN(THT)
2030 CH=COS(THT)
2040 AST=RA*SH
2050 SS=AST/RS
2060 IF SS>1 THEN 2090
2070 CS=SQR(1-SS*SS)
2080 GOTO 2110
2090 TBS=1
2100 CS=SQR(SS*SS-1)
2110 REM  PHASE THICKNESS
2120 IF N=0 THEN 2190
2130 FOR J=1 TO N
2140 SJ=AST/R(J)
2150 CJ(J)=SQR(1-SJ*SJ)
2160 Z(J)=X(J)
2170 X(J)=Z(J)*CJ(J)
2180 NEXT J
2190 AIR=RA
2200 SUB=RS
2210 REM  S COMPONENT OF POLARIZATION
2220 SN=0
2230 RA=AIR*CH
2240 RS=SUB*CS
2250 IF N=0 THEN 2300
2260 FOR J=1 TO N
2270 R1(J)=R(J)
2280 R(J)=R1(J)*CJ(J)
2290 NEXT J
2300 GOSUB 3000
2310 FOR IA=1 TO M
2320 SR(IA)=REF(IA)
2330 ST(IA)=TS(IA)
2335 NEXT IA
2340 REM  P-COMPONENT OF POLARIZATION
2350 SN=1
2360 RA=AIR/CH
2370 RS=SUB/CS
2380 IF N=0 THEN 2420
2390 FOR J=1 TO N
2400 R(J)=R1(J)/CJ(J)
2410 NEXT J
2420 GOSUB 3000
```

```
2430 FOR IA=1 TO M
2440 PR(IA)=REF(IA)
2450 PT(IA)=TS(IA)
2460 REF(IA)=0.5*(SR(IA)+PR(IA))
2470 TS(IA)=0.5*(ST(IA)+PT(IA))
2480 NEXT IA
2490 IF N=0 THEN 2540
2500 FOR J=1 TO N
2510 X(J)=Z(J)
2520 R(J)=R1(J)
2530 NEXT J
2540 RA=AIR
2550 RS=SUB
2560 RETURN
3000 FOR IA=1 TO M
3010 IF N=0 THEN 3230
3020 P1=/180*X(1)*FRQ(IA)
3030 B1=COS(P1)
3040 B2=SIN(P1)/R(1)
3050 C1=B2*R(1)*R(1)
3060 C2=B1
3070 IF N=1 THEN 3270
3080 FOR J=2 TO N
3090 P1=/180*X(J)*FRQ(IA)
3100 D1=COS(P1)
3110 D2=SIN(P1)/R(J)
3120 E1=D2*R(J)*R(J)
3130 E2=D1
3140 A1=B1*D1-B2*E1
3150 A2=B1*D2+B2*E2
3160 Z1=C1*D1+C2*E1
3170 Z2=C2*E2-C1*D2
3180 B1=A1
3190 B2=A2
3200 C1=Z1
3210 C2=Z2
3215 NEXT J
3220 GOTO 3270
3230 B1=1.0
3240 B2=0.0
3250 C1=0.0
3260 C2=0.0
3270 IF TBS=1 THEN 3370
3280 NR=B1*AIR-C2*SUB
3290 NI=B2*AIR*SUB-C1
3300 DR=B1*AIR+C2*SUB
3310 DI=B2*AIR*SUB+C1
3320 EH=NR*NR+NI*NI
3330 PH=DR*DR+DI*DI
3340 REF(IA)=EH/PH
3350 TS(IA)=1-REF(IA)
3360 GOTO 3400
3370 REF(IA)=1.0
3380 TS(IA)=0.0
3400 NEXT IA
3410 RETURN
```

REFLECTION, TRANSMISSION, AND ABSORPTION
VALUES CALCULATED FOR A 100A SILVER FILM

W(NM)	R (%)	T (%)	A (%)
400	.142	.831	.026
450	.188	.791	.020
500	.235	.746	.018
550	.286	.693	.020
600	.335	.643	.021
650	.387	.588	.023
700	.433	.543	.023
750	.478	.498	.023
800	.514	.460	.024
850	.548	.425	.025
1250	.589	.342	.067
1500	.638	.292	.068
2000	.749	.186	.064
3000	.837	.096	.065

```
1 OPEN4,4:CMD4
2 PRINT "REFLECTION, TRANSMISSION, AND ABSORPTION"
3 PRINT "VALUES CALCULATED FOR A 100A SILVER FILM"
4 PRINT
7 PRINT "W(NM)","R (%)","T (%)","A (%)"
10 READ W,N,K
20 W=W*1E-7
30 A=4*3.141592654*N*1E-8/W
40 X=4*3.141592654*K*1E-8/W
50 A1=((1-N)^2+K^2)*((N+1.52)^2+K^2)
60 A2=((1+N)^2+K^2)*((N-1.52)^2+K^2)
70 A3=2*((1-(N^2+K^2))*(N^2+K^2-1.52^2)+4*K*(-1.52*K))
80 A4=4*((1-N^2-K^2)*(-1.52*K)-K*(N^2+K^2-2.31))
90 B1=((1+N)^2+K^2)*((N+1.52)^2+(K)^2)
100 B2=((1-N)^2+K^2)*((N-1.52)^2+(K)^2)
110 B3=2*((1-N^2-K^2)*(N^2+K^2-2.31)-4*K*(-1.52*K))
120 B4=4*((1-N^2-K^2)*(-1.52*K)+K*(N^2+K^2-2.31))
130 R=(A1*EXP(X)+A2*EXP(-X)+A3*COS(A)+A4*SIN(A))
135 R=R/(B1*EXP(X)+B2*EXP(-X)+B3*COS(A)+B4*SIN(A))
138 PRINT W/1E-9,
140 R$=STR$(R)
145 PRINT LEFT$(R$,5),
150 T=16*1.52*(N^2+K^2)
160 T=T/(B1*EXP(X)+B2*EXP(-X)+B3*COS(A)+B4*SIN(A))
170 T$=STR$(T)
175 PRINT LEFT$(T$,5),
180 P=1-T-R
190 P$=STR$(P)
192 PRINT LEFT$(P$,5)
195 IF K=18.2 THEN 600
200 GOTO 10
500 DATA 4,.075,1.93,4.5,.055,2.42,5,.05,2.87,5.5,.055,3.32,6,.06,3.75
510 DATA 6.5,.07,4.2,7,.075,4.62,7.5,.08,5.05,8,.09,5.45,8.5,.1,5.85
520 DATA 12.5,.37,7.7,15,.45,9,20,.65,12.2,30,1.3,18.2
600 CLOSE4
620 END
```